Technical Note

1975-1

R. L. Harvey

Spacecraft Self-Contamination by Molecular Outgassing

31 March 1975

Prepared for the Department of the Air Force
under Electronic Systems Division Contract F19628-73-C-0002 by

Lincoln Laboratory
MASSACHUSETTS INSTITUTE OF TECHNOLOGY
LEXINGTON, MASSACHUSETTS

The work reported in this document was performed at Lincoln Laboratory, a center for research operated by Massachusetts Institute of Technology, with the support of the Department of the Air Force under Contract F19628-73-C-0002.

This technical report has been reviewed and is approved for publication.

FOR THE COMMANDER

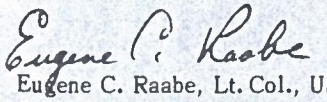

Eugene C. Raabe, Lt. Col., USAF
Chief, ESD Lincoln Laboratory Project Office

MASSACHUSETTS INSTITUTE OF TECHNOLOGY
LINCOLN LABORATORY

SPACECRAFT SELF-CONTAMINATION BY MOLECULAR OUTGASSING

R. L. HARVEY
Group 67

TECHNICAL NOTE 1975-1

31 MARCH 1975

LEXINGTON MASSACHUSETTS

ABSTRACT

The contamination of spacecraft surfaces from ambient and outgassing molecules is considered. A model is formulated for the molecules desorbed from the spacecraft surfaces and scattered by the ambient molecules back to the emitting and adjacent surfaces. Equations are derived for the backscatter and far-field cases as a function of surface geometry, mean free path, and desorbing beam shape. Expressions are given for point to point and flat surface to point scattering. The scattered molecular irradiance is combined with other sources to obtain the total molecular irradiance. A calculation of the contamination during launch of the Lincoln Experimental Satellites 8 and 9 is given.

TABLE OF CONTENTS

List of Figures

List of Tables

I. INTRODUCTION

Spacecraft contamination due to the adherence of molecules on external surfaces can in some instances be important to the mission success. It is well known that the buildup of molecular layers can change the radiometric coefficients of a surface. The transmittance and reflectance of optical surfaces may be adversely changed in terms of both spectral and directional characteristics. The emissivity, absorptivity, and reflectivity of nonoptical surfaces are also affected by surface films. These films, if present, must be included in the design of thermal control systems and sensors.

In this Technical Note analytic models have been developed for estimating the molecular irradiance (molecules cm^{-2}) on a spacecraft surface due to molecules desorbed (emitted) from adjacent surfaces and scattered by ambient molecules to the receiving surface. The total irradiance on a receiving area (A_r) due to molecules outgassing from an emitting area (A_e) and from irradiating ambient molecules in the free stream has been schematically shown in Fig. I-1. In general, the irradiance can come by four paths:

(1) Direct irradiance: molecules are desorbed from A_e and go directly to A_r. In this case the surfaces must "see" each other and their normals must satisfy the condition $\vec{e}_e \cdot \vec{e}_r > 0$.

(2) Scattered irradiance: molecules are desorbed from A_e and are scattered by another surface or other molecules to A_r. Models for scattering by ambient molecules have been developed in this Technical Note.

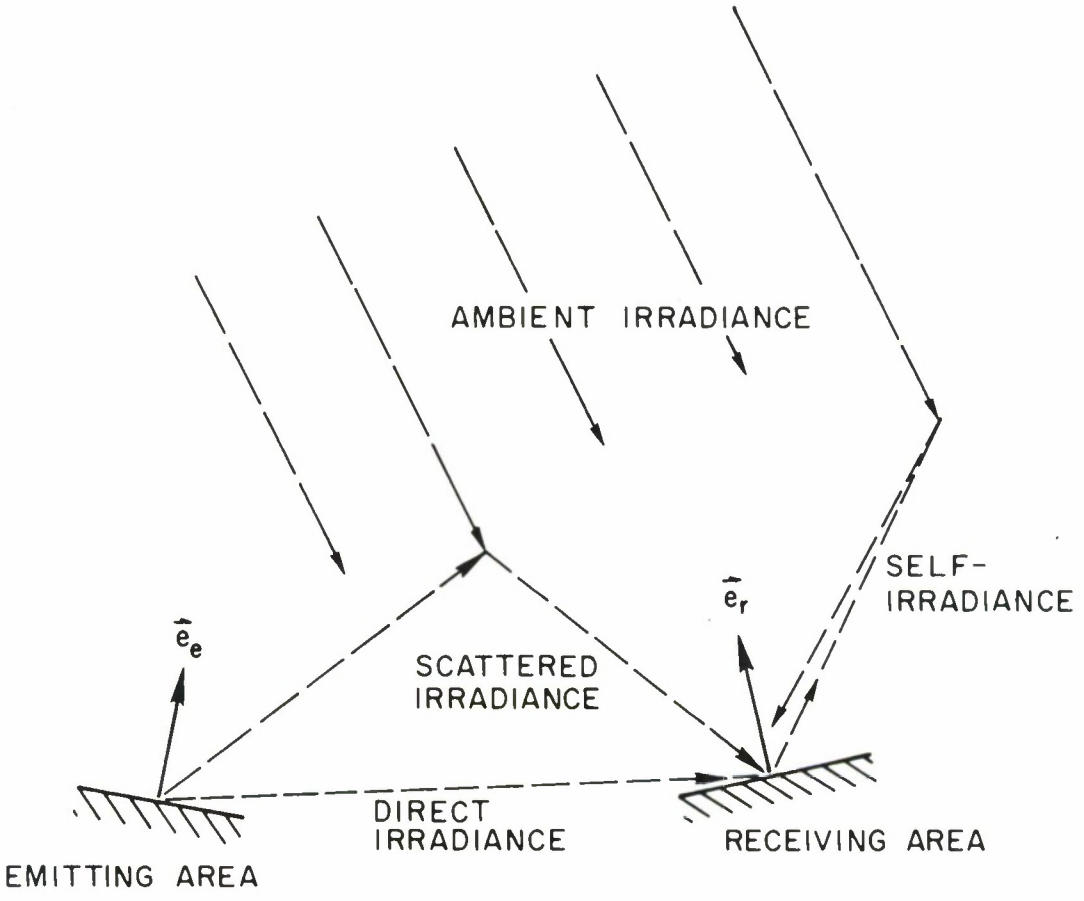

Fig. I-1. Molecular irradiance paths.

(3) Self irradiance: molecules are desorbed by A_r and then scattered back to A_r. Models for this path have been also developed.

(4) Ambient irradiance: A_r is bombarded by free stream molecules.

While the scattering of molecular beams by molecules and surfaces has been intensively investigated both theoretically and experimentally, little work has been done on molecular exchanges between adjacent surfaces by scattering with intervening molecules. Scialdone[1,2] has developed an analytic model for the self-contamination of a spherical spacecraft due to the outgassing of molecules which are scattered back to the emitting surface (path 3). In the present analysis this path has been considered as the special case of the emitting and receiving areas coinciding. Scialdone assumed a simple scattering model for the desorbed ambient molecular collisions. A more realistic, but still approximate, isotropic scattering model has been introduced in the present analysis and it is shown to give an upper bound on non-isotropic scattering. Also, it is shown that for certain cases the present model and Scialdone's model give identical results. Lee, et al.[3] reported a Monte Carlo computer program for calculating molecular fluxes within vacuum chambers. The program considered only scattering by the chamber walls and is not applicable to the problem of scattering by intervening molecules. The problem of test chamber contamination has also been considered by Scialdone[2] using his backscatter model.

In Section II a general equation is derived for the molecular irradiance assuming single isotropic collisions. The resulting volume integral is evaluated in Section III for the backscatter case (path 3) and is compared with

Scialdone's model. In Section IV the farfield solution is obtained for the irradiance. The resulting elementary area solution is integrated to get the irradiance at a point due to outgassing from an adjacent planar area. A summary of the assumptions and formulas is given in Section V. The resulting analytic models are used in Section VI for estimating the contamination on the Lincoln Experimental Satellites (LES) 8 and 9 due to desorbed molecules from the Transtage launch vehicle during boost to orbit. Finally, computational details have been collected in the Appendices.

II. IRRADIANCE FROM SCATTERED MOLECULES

As shown in Fig. I-1 the molecular irradiance on a surface may come from ambient molecules directly impacting on the surface or from adjacent outgassing molecules traveling directly to the surface or, thirdly, from adjacent outgassing molecules which have been scattered one or more times before impinging on the surface. In any particular situation several of these irradiance paths may be present. The non-scattered components of the total irradiance are known once the surface ourgassing rates, ambient molecular fluxes, and the geomtry are given. The scattered component is more complex because of the multitude of paths each molecule can take, the details of the collision processes, and geometry factors such as shadowing. As a first approximation it will be assumed that the molecules scattered to a surface undergo only one collision with an intervening ambient molecule after being desorbed from an adjacent surface. This model is applicable to the low density regime where the Knudsen number (λ/ℓ) is large. The collision processes are approximated by isotropic scattering in a reference frame attached to the emitting surface (laboratory frame).

This assumption simplifies the general equation in Section II.A; as discussed in Section II.B, isotropic scattering also gives an upper bound on non-isotropic scattering in the upstream direction.

A. Isotropic Scattering

Consider an area (A_e) emitting molecules into the solid angle $d\omega$ (Fig. II-1). By definition of the specific intensity (I)*, the rate of molecules leaving A_e in direction $\vec{e}_\omega$ is

$$= I\, A_e \cos\theta_e d\omega. \quad (\text{molecules sec}^{-1}) \tag{1}$$

The total emitted molecular flux (N) leaving A_e is

$$N = \int_{\omega \leq 2\pi} I_e \cos\theta_e d\omega. \quad (\text{molecules sec}^{-1}\text{cm}^{-2}) \tag{2}$$

For a diffuse or Lambertian surface emitting into a conical beam defined by the semi-vertex angle θ**, Eq. (2) becomes

$$N = \pi I \sin^2\theta, \quad 0 < \theta \leq \pi/2. \tag{3}$$

Let the scattering of the emitted molecules be characterized by the mean free path (λ). The probability of a molecule traveling a distance r_e without being

---

* The nomenclature has been based on radiometric symbols with molecules used in place of photons.[4]

** The reason for considering this more general case is that certain integrals are undefined at $\theta=\pi/2$ and, hence, θ must be restricted.

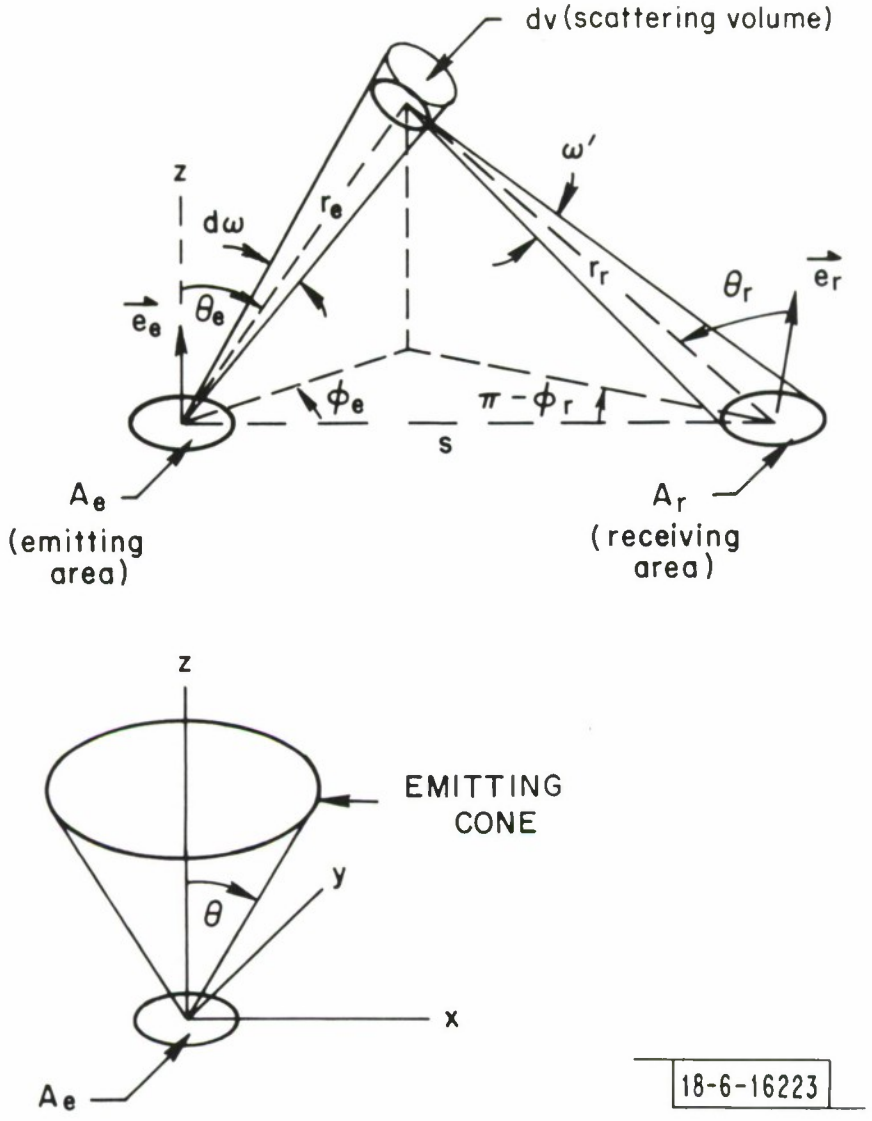

Fig. II-1. Nomenclature for single scattering analysis

scattered is by definition of λ given by $\exp(-\frac{r_e}{\lambda})$. The number of molecules per second which leave A_e in $d\omega$ and arrive at distance r_e is therefore

$$= I\, A_e \cos\theta_e\, d\omega\, \exp(-\frac{r_e}{\lambda}) . \qquad (4)$$

The fraction of these molecules scattered in distance dr_e is $\frac{dr_e}{\lambda}$, hence, the molecules per second scattered in dr_e is

$$= I\, A_e \cos\theta_e\, d\omega\, \exp(-\frac{r_e}{\lambda})\frac{dr_e}{\lambda} . \qquad (5)$$

The scattered molecules in general leave $d\omega$ and travel in a new direction. Assuming isotropic scattering in the laboratory frame, the number of molecules per second entering ω' is

$$= I\, A_e \cos\theta_e\, d\omega\, \exp(-\frac{r_e}{\lambda})\frac{dr_e}{\lambda}\frac{\omega'}{4\pi} . \qquad (6)$$

When ω' is defined to contain the receiving area A_r (Fig. II-1), the molecular irradiance (H) on A_r, assuming no further scattering, is

$$dH = I\,\frac{A_e}{A_r}\cos\theta_e\, d\omega\, \exp(-\frac{r_e}{\lambda})\frac{dr_e}{\lambda}\frac{\omega'}{4\pi} . \quad (\text{molecules sec}^{-1}\text{cm}^{-2}) \qquad (7)$$

Noting that $d\omega\, dr_e = \frac{dv}{r_e^2}$, where dv is the differential scattering volume, Eq. (7) becomes

$$dH = \frac{I}{4\pi} \frac{A_e}{A_r} \cos\theta_e \exp\left(-\frac{r_e}{\lambda}\right) \frac{dv}{\lambda r_e^2} \omega' . \tag{8}$$

Equation (8) must be integrated over the volume (V) defined by the emitting beam ($0 < \theta \leq \frac{\pi}{2}$) and the condition that $\theta_r \leq \pi/2$ (disregarding shadowing). The total irradiance becomes

$$H = \frac{I}{4\pi} \frac{A_e}{A_r} \iiint_V \cos\theta_e \exp\left(-\frac{r_e}{\lambda}\right) \frac{dv}{\lambda r_e^2} \omega' . \tag{9}$$

In spite of the simple model used in its derivation, Eq. (9) is difficult to evaluate for general orientations between the emitting and receiving areas. The volume V over which Eq. (9) is integrated has been indicated in Fig. II-2. The following sections evaluate Eq. (9) for particular cases of interest.

B. Nonisotropic Scattering

Appendix A summarizes briefly the theory of binary molecular collisions. For an elastic collision between two smooth spheres (adiabatic collision) it is shown that the scattering of both spheres is isotropic with respect to a center of mass coordinate system. Figure II-3 shows the scattering distribution of a desorbed molecule after collision with an ambient molecule when both molecules have been approximated by perfectly elastic, smooth spheres. It can be seen that the scattering in a reference frame attached to the emitting area (laboratory frame) is nonisotropic while being isotropic in a center of mass frame. As intuitively expected, Fig. II-3 shows that more desorbed molecules are scattered downstream in the direction of the ambient

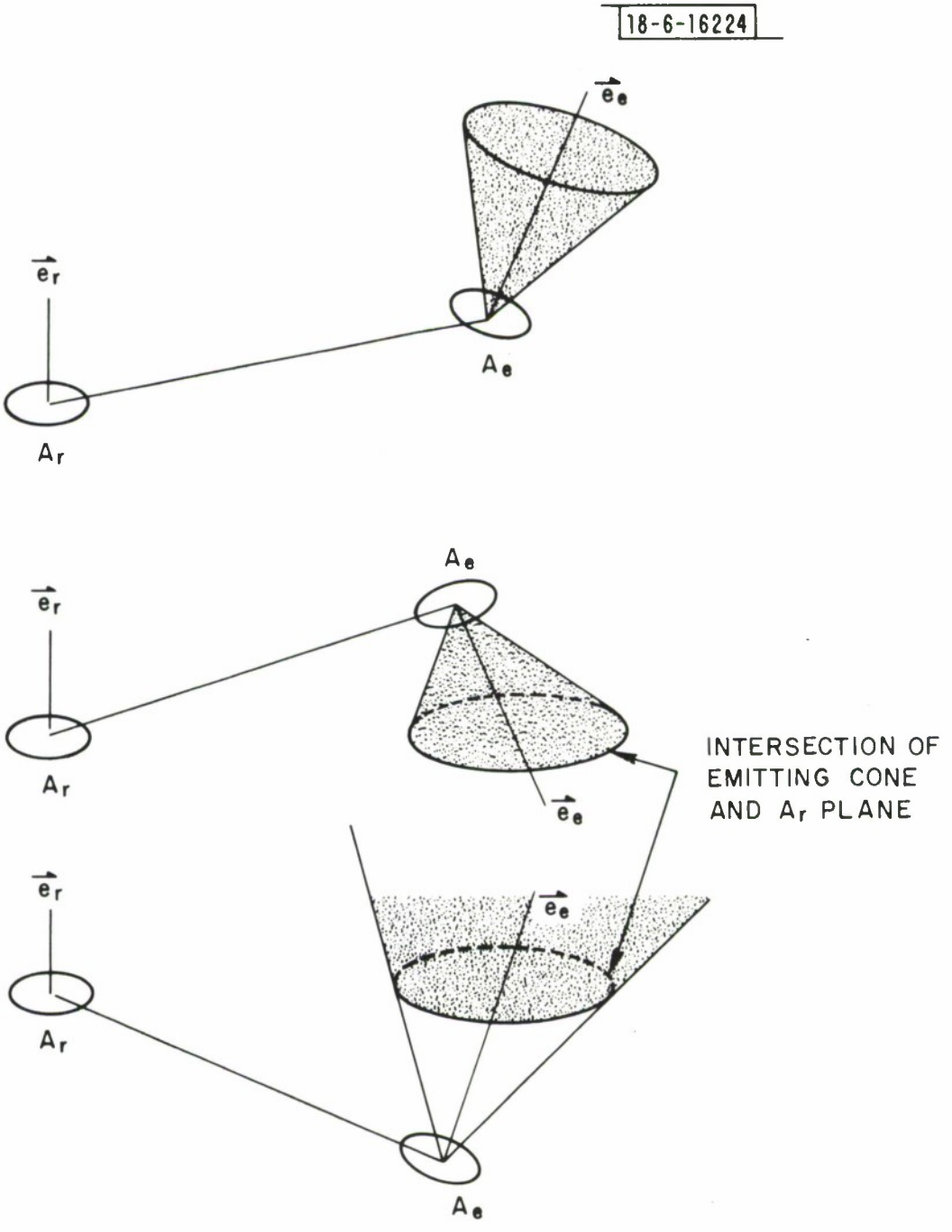

Fig. II-2. Integration volumes.

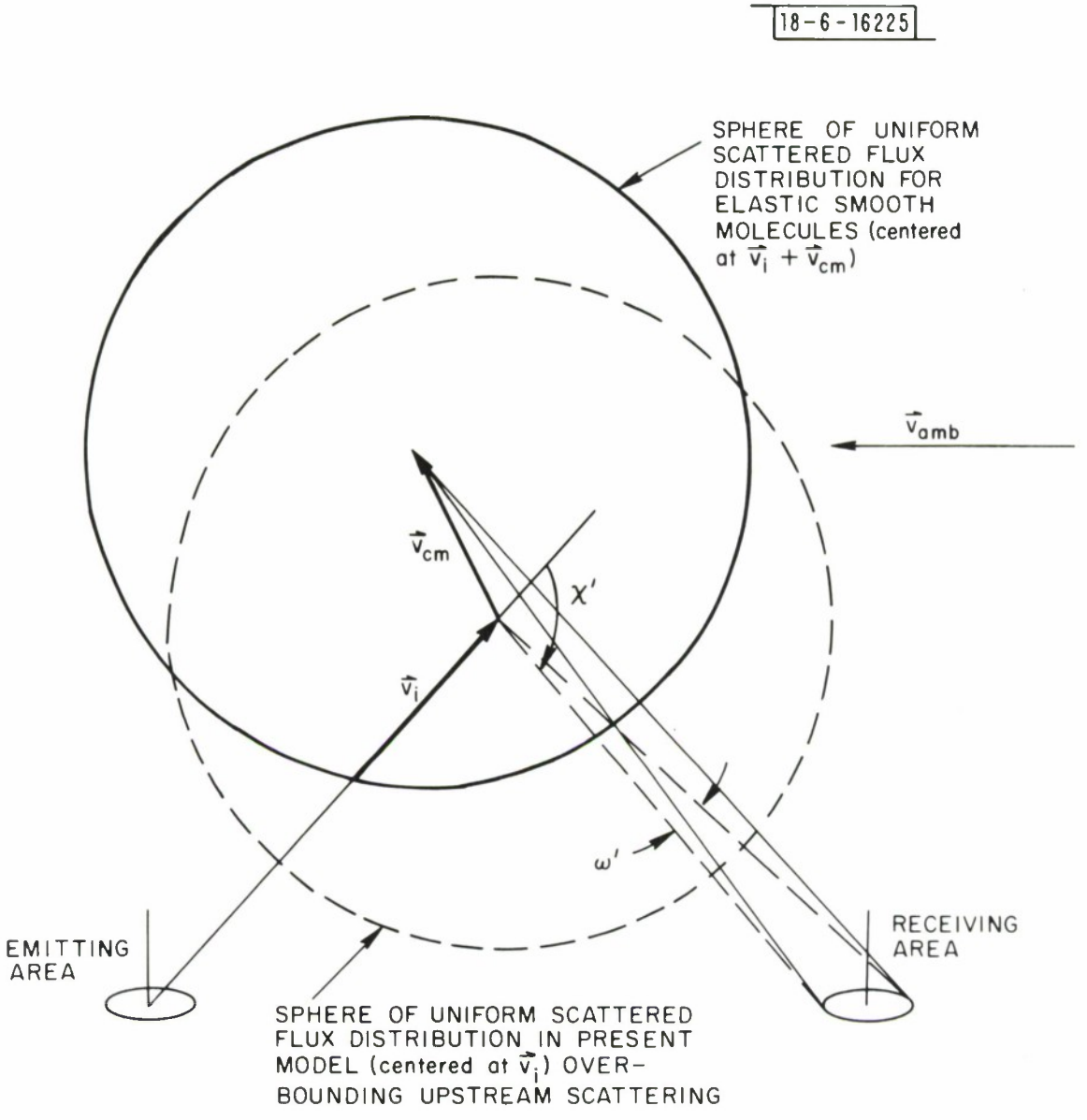

Fig. II-3. Scattering distribution of two smooth spheres.

motion than is given by an isotropic distribution in the laboratory frame. In Section A the fraction of molecules scattered into a particular solid angle ω' with respect to a laboratory reference frame has been approximated by the isotropic distribution $\frac{\omega'}{4\pi}$. The distribution $\frac{\omega'}{4\pi}$ will give an upper bound on the number of molecules scattered upstream and underestimates the number scattered downstream; hence, the irradiance on an area upstream of an emitting area is upper bounded by Eq. (9). The nonisotropy caused by non-spherical molecules is difficult to estimate; however, this effect should not increase the scattering in the upstream direction so that Eq. (9) remains an upper bound on the upstreams irradiance.

III. BACKSCATTER SOLUTIONS

A. Cylindrical Beam Backscattering

Letting

$$dv = r_e^2 \, dr_e d\omega,$$

and

$$\frac{A_e}{A_r} = 1, \tag{10}$$

Eq. (9) can be written as

$$H = \frac{I}{4\pi} \int_0^\infty d(\tfrac{r}{\lambda}) \, \exp(-\tfrac{r}{\lambda}) \omega' \int_{\omega(r)} \cos\theta_e d\omega. \tag{11}$$

Assuming that all the outgassing molecules are confined to a narrow cylindrical beam, the molecular flux N leaving the emitting area (A) is

$$N = I \int_{\omega(r)} \cos\theta_e \, d\omega, \tag{12}$$

where $\omega(r)$ is the solid angle enclosing the beam. The fraction of the molecules isotropically scattered directly back to the emitting surface is from Eq. (11)

$$\frac{H}{N} = \frac{1}{4\pi} \int_0^\infty d\left(\frac{r}{\lambda}\right) \exp\left(-\frac{r}{\lambda}\right) \omega'. \tag{13}$$

The scattering solid angle ω' can be written for all values of r as

$$\omega' = 2\pi(1 - \cos\gamma), \tag{14}$$

where

$$\cos\gamma = \frac{r}{(r^2 + \rho^2)^{1/2}}, \tag{15}$$

$$\pi\rho^2 = A. \tag{16}$$

As expected, for r large, $\omega' \approx \frac{A}{r^2}$ and for r small $\omega' \approx 2\pi$.

Equation (13) is nondimensionalized by

$$x = \frac{r}{\lambda},$$

$$\varepsilon = \frac{\rho}{\lambda} . \tag{17}$$

Equation (13) can be written

$$\frac{H}{N} = \frac{I_1(\varepsilon)}{2} , \tag{18}$$

where

$$I_1(\varepsilon) = \int_0^\infty dx \exp(-x)\left[1 - \frac{x}{(x^2+\varepsilon^2)^{1/2}}\right] . \tag{19}$$

For ε small, it can be shown (Appendix B) that $I_1(\varepsilon) \approx \varepsilon$.* After the indicated substitutions, Eq. (18) becomes

$$\frac{H}{N} \approx \left(\frac{A}{4\pi\lambda^2}\right)^{1/2} , \quad \frac{A}{\lambda^2} << 1. \tag{20}$$

Scialdone[1] considered molecules radially leaving a spherical spacecraft (radius R) and being scattered back toward the emitting surface. Molecules scattered out of the emitting column were disregarded under the assumption that

---

* For arbitrary ε the exact solution is a function of the Struve and Neuman functions of the first kind.[5] For ε small $I(\varepsilon)$ is determined by the integrand near x=0; hence, bounding exp(-x) by unity and integrating gives the first term in the expansion of the exact solution.

they are replaced by molecules scattered in from other columns. In his notation, the returning flux N" as a function of the number of original molecules per second coming from the surface N_D is

$$N'' = \frac{N_D}{4\pi\lambda R} \quad , \quad \lambda >> R. \tag{21}$$

The departing flux N would be $\frac{N_D}{4\pi R^2}$ yielding a flux ratio of

$$\frac{N''}{N} = \frac{R}{\lambda} \tag{22}$$

Using Eq. (20) and neglecting scattering from other beam columns, the flux ratio over a spherical spacecraft also becomes $\frac{R}{\lambda}$ agreeing with Scialdone's result. A more precise analysis taking into account the contribution from other beams would increase the flux ratios over this result. This extension is difficult as will become apparent from considering the scattering between two surface elements.

B. Conical Beam Backscattering

Beginning with Eq. (9) with $A_e = A_r$, the self-irradiance of a surface becomes

$$H = \frac{I}{4\pi} \iiint_V \cos\theta_e \exp(-\frac{r}{\lambda}) \frac{dv}{\lambda r^2} \omega'. \tag{23}$$

The integration volume V is the entire emitting cone. Following the approach of the preceeding section let

$$dv = r^2 \sin\theta_e \, d\theta_e d\phi_e dr$$

$$\omega' = 2\pi \left[1 - \frac{r}{(r^2+\gamma^2)^{1/2}}\right]$$

$$\pi\gamma^2 = A \cos\theta_e \quad . \tag{24}$$

Non-dimensionizing as before, Eq. (23) becomes

$$H = \pi I \int_0^{\theta} d\theta_e \cos\theta_e \sin\theta_e I_2(\varepsilon, \theta_e) \tag{25}$$

where

$$I_2(\varepsilon, \theta_e) = \int_0^{\infty} dx \exp(-x) \left[1 - \frac{x}{(x^2+\varepsilon^2\cos\theta_e)^{1/2}}\right] \quad . \tag{26}$$

By arguments similar to those used in approximating $I_1(\varepsilon)$, $I_2(\varepsilon, \theta_e)$ becomes

$$I_2(\varepsilon, \theta_e) \approx \varepsilon \cos^{1/2}\theta_e \quad . \tag{27}$$

Equation (25) becomes

$$H \approx \frac{2}{5} (1 - \cos^{5/2}\theta) \, I \left(\frac{\pi A}{\lambda^2}\right)^{1/2} \tag{28}$$

Using Eq. (3)

$$\frac{H}{N} \approx \frac{2}{5} \frac{(1-\cos^{5/2}\theta)}{\sin^2\theta} \left(\frac{A}{\pi\lambda^2}\right)^{1/2} \quad , \frac{A}{\lambda^2} << 1. \tag{29}$$

Two limiting values for Eq. (29) are the cylindrical solution $\theta \to 0$

$$\frac{H}{N} = \left(\frac{A}{4\pi\lambda^2}\right)^{1/2} \quad , \ \theta = 0, \tag{30}$$

and the hemispherical solution

$$\frac{H}{N} = \frac{4}{5}\left(\frac{A}{4\pi\lambda^2}\right)^{1/2} \quad , \ \theta = \pi/2 \tag{31}$$

A conical beam thus produces 20% less backscattering than a cylindrical beam with the same emitted molecular flux.

IV. FARFIELD SOLUTIONS

The nomenclature for scattering between different elementary surfaces has been shown in Fig. IV-1. The solid angle (ω') into which the desorbed molecules are scattered after collision with an ambient molecule is, in general, given by expressions similar to Eqs. (14) and (24). A simplification is possible if ω' is restricted to the farfield. In this limit

$$\omega' \approx \frac{A_r \cos\theta_r}{r_r^2}$$

and

$$\frac{A_r}{r_r^2} \ll 1. \tag{32}$$

Defining the nondimensional quantities

$$X = \frac{r_e}{\lambda} \quad ,$$

$$y = \frac{r_r}{\lambda} \quad ,$$

$$S = \frac{s}{\lambda} \quad , \tag{33}$$

from Fig. IV-1, $\cos\theta_r$ can be written as

$$\cos\theta_r = \frac{S}{y}\vec{e}_s \cdot \vec{e}_r + \frac{x}{y}\vec{e}_\omega \cdot \vec{e}_r, \tag{34}$$

where

$$y^2 = x^2 + S^2 + 2xS\,\vec{e}_\omega \cdot \vec{e}_s \; . \tag{35}$$

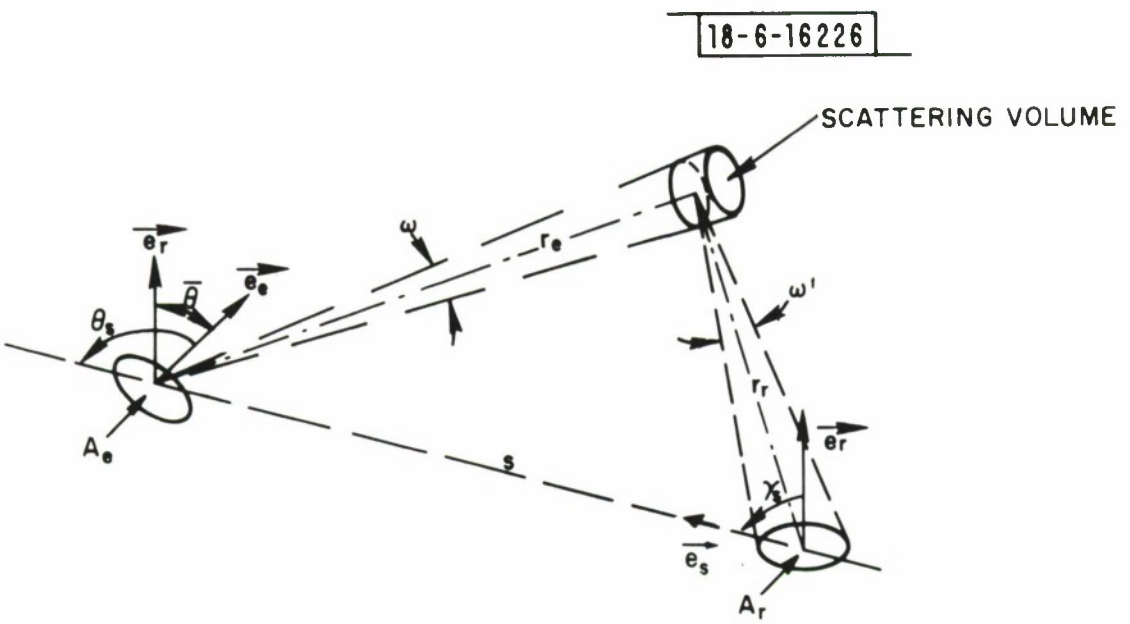

Fig. IV-1. Orientation between two elementary surfaces.

Substituting Eqs. (32) - (35) in Eq. (9) gives

$$H = \frac{IA_e}{4\pi\lambda^2} \iiint_V d\omega\, dx \cos\theta_e \exp(-x) \left(\frac{S}{y^3} \vec{e}_s \cdot \vec{e}_r + \frac{x}{y^3} \vec{e} \cdot \vec{e}_r\right). \quad (36)$$

The volume (V) is the emitting cone for which $\cos \theta_r \geq 0$. Shadowing by other surfaces has been disregarded, but could be included if necessary.

A. Arbitrary Orientations Between Elementary Surfaces

When the volume of integration is the entire emitting cone, then Eq. (36) can be written as

$$H = \frac{IA_e}{4\pi\lambda^2} \iint d\omega \cos\theta_e \, (I_3 + I_4) \, , \quad (37)$$

where

$$I_3 = S \, \vec{e}_s \cdot \vec{e}_r \int_o^\infty dx \, \frac{\exp(-x)}{y^3} \, , \quad (38)$$

$$I_4 = \vec{e}_\omega \cdot \vec{e}_r \int_o^\infty dx \, \frac{x \exp(-x)}{y^3} \, . \quad (39)$$

As in the backscatter solutions, it has been shown in Appendix B that bounding exp (-x) by unity gives a tight bound for $\frac{A_r}{\lambda^2} << 1$.

Eqs. (38) and (39) can be integrated to give

$$I_3 \approx \frac{\vec{e}_s \cdot \vec{e}_r}{S(1 + \vec{e}_\omega \cdot \vec{e}_s)} \, , \quad (40)$$

$$I_4 \approx \frac{\vec{e}_\omega \cdot \vec{e}_r}{S(1 + \vec{e}_\omega \cdot \vec{e}_s)} \quad (41)$$

The farfield solution becomes

$$H = \frac{IA_e}{4\pi\lambda s} \iint d\omega \cos\theta_e \frac{(\vec{e}_s \cdot \vec{e}_r + \vec{e} \cdot \vec{e}_r)}{(1 + \vec{e}_\omega \cdot \vec{e}_s)} \quad . \tag{42}$$

As shown in Fig. IV-1 the orientation between two surfaces can be uniquely described by the distance between them (s) and the three angles γ_s, θ_s and $\bar{\theta}$. In order that the integration be over the entire emitting cone, the emitting surface must be above the receiving surface, as indicated in Fig. II-2, and the emitting cone must be restricted so that the farfield assumption $\frac{A_r}{r^2} << 1$ holds over the entire integration range. Under these limitations, it has been shown in Appendix B that starting with Eq. (42) the integration over the entire emitting cone gives

$$\frac{H}{N} = \frac{1}{4\pi} \frac{A_e}{\lambda s} f, \tag{43}$$

where

$$f = \frac{\cos \bar{\theta} + \cos \gamma_s}{1 + \cos \theta_s} \tag{44}$$

This result is independent of the emitting cone angle (θ).

There are maximum and minimum value of $\bar{\theta}$ which are functions of θ_s and γ_s. A consideration of the possible orientations of A_e with respect to A_r gives

$$\bar{\theta}_{min} = \gamma_s - \theta_s, \quad \theta_s \leq \gamma_s,$$

$$\bar{\theta}_{min} = \theta_s - \gamma_s, \quad \theta_s \geq \gamma_s,$$

$$\bar{\theta}_{max} = \gamma_s + \theta_s, \quad \theta_s + \gamma_s \leq \pi,$$

$$\bar{\theta}_{max} = 2\pi - (\gamma_s + \theta_s), \quad \theta_s + \gamma_s \geq \pi. \tag{45}$$

The farfield assumption $(\frac{A_r}{r_r^2} << 1)$ can be written using

$$\frac{A_r}{r_r^2} \leq \frac{A_r}{(r_r)^2_{min}}$$

and

$$(r_r)_m = s \sin(\theta + \theta_s) ,$$

so

$$\frac{A_r}{s^2 \sin^2(\theta + \theta_s)} << 1.$$

Figures IV-2 and IV-3 show the function f for several values of γ_s. As γ_s approaches 0°, f approaches unity and H/N becomes independent of the surface orientations corresponding to the emitting surface being directly above the receiving surface.

B. Plane to Coplanar Point

The farfield elementary area solution, Eq. (43), can be applied to find the molecular irradiance at a point due to desorption from an adjacent coplanar area. Figure IV-4 shows the nomenclature for a flat, rectangular surface (A) emitting molecules which are scattered to a single coplanar point. In this case

$$\gamma_s = \theta_s = \pi/2$$

$$\bar{\theta} = 0,$$

and

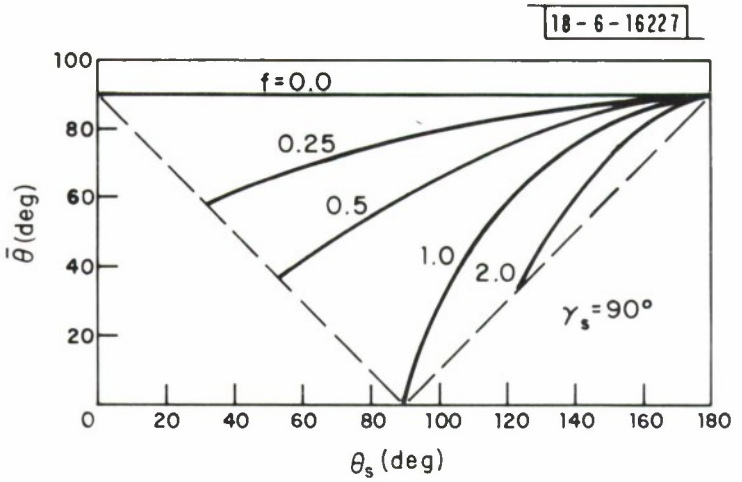

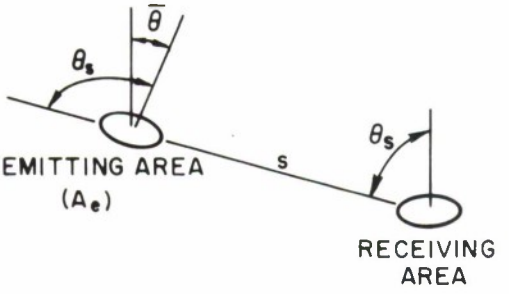

$$\frac{H}{N} = \frac{A_e f}{4\pi\lambda s}$$

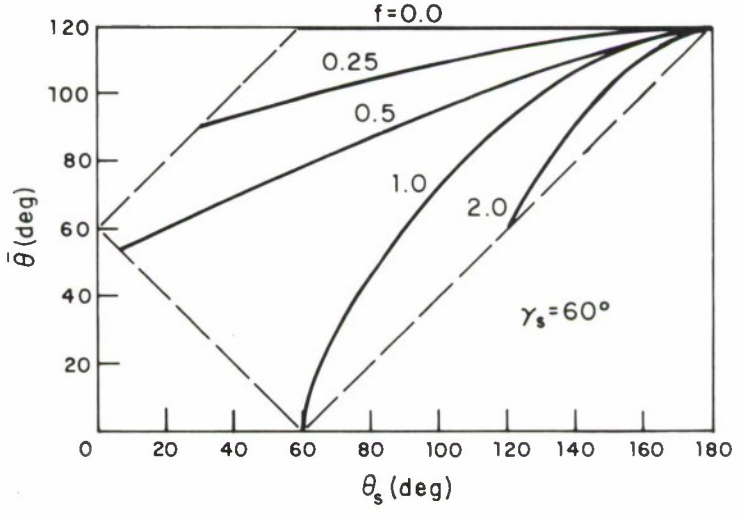

Fig. IV-2. f as a function of θ_s and $\bar{\theta}$ (γ_s = 90°, 60°).

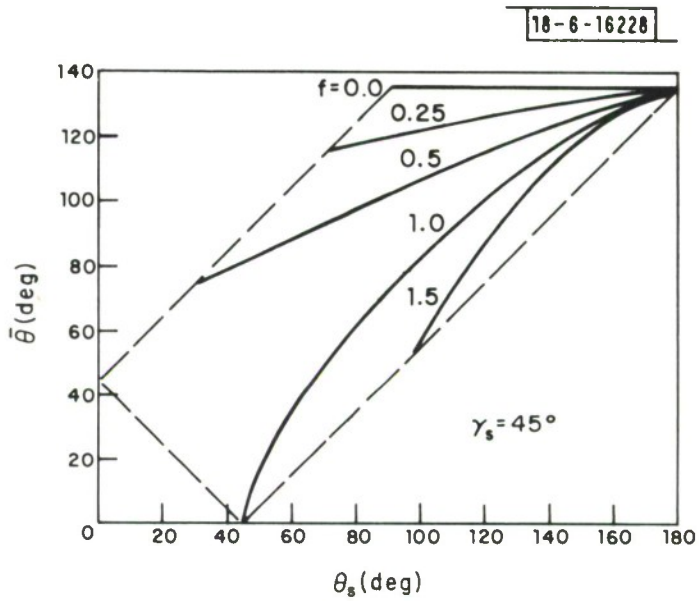

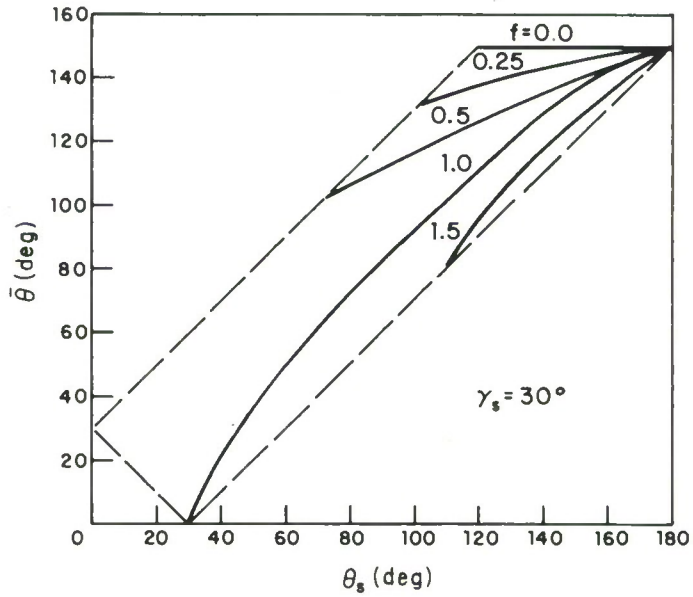

Fig. IV-3. f as a function of θ_s and $\bar{\theta}$ (γ_s = 45°, 30°).

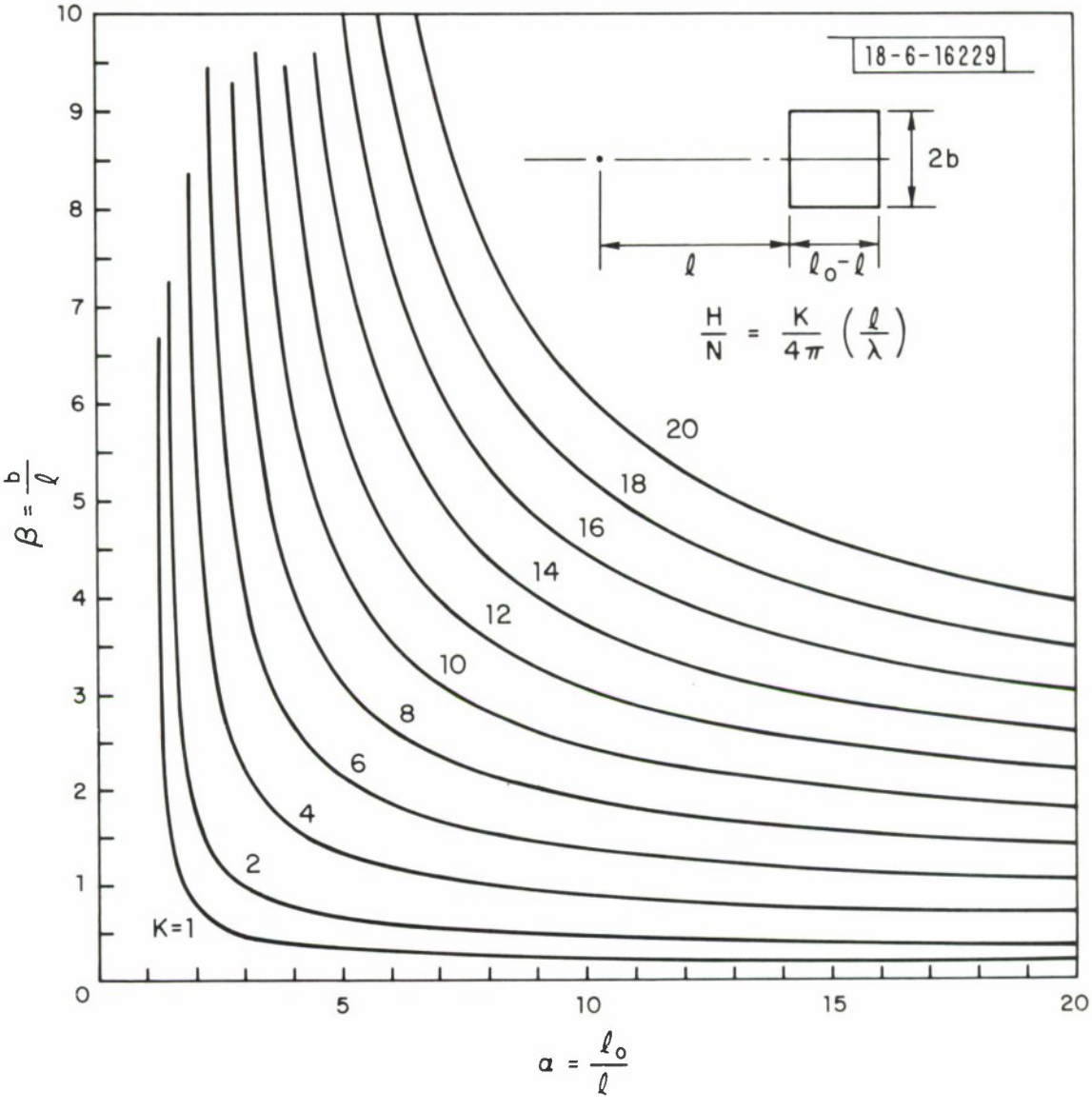

Fig. IV-4. Scattering from a plane to a coplanar point.

$$f = 1 \tag{46}$$

Eq. (43) gives

$$\frac{H}{N} = \frac{1}{4\pi\lambda} \iint_A \frac{dA}{s} . \tag{47}$$

Eq. (47) can be written as

$$H = \frac{N}{4\pi} \left(\frac{\ell}{\lambda}\right) K(\alpha,\beta), \tag{48}$$

where

$$K(\alpha,\beta) = \int_{1-1}^{\alpha}\int^{1} \frac{dx\ dy}{(x^2 + \beta^2\ y^2)^{1/2}} ,$$

$$\alpha = \frac{\ell_o}{\ell} ,$$

$$\beta = \frac{b}{\ell} . \tag{49}$$

The integration of Eq. (49) gives

$$K(\alpha,\beta) = \alpha \ell n \left[\frac{\beta + (\alpha^2+ \beta^2)^{1/2}}{-\beta + (\alpha^2+ \beta^2)^{1/2}}\right] - \ell n \left[\frac{\beta + (1+ \beta^2)^{1/2}}{-\beta + (1+ \beta^2)^{1/2}}\right] + 2\beta \ell n \left[\frac{\alpha + (\alpha^2+ \beta^2)^{1/2}}{1 + (1+\beta^2)^{1/2}}\right] \tag{50}$$

Note that in the limit of $\alpha \to 1$ and $\beta \to 0$, Eq. (50) gives, as expected, $K(\alpha,\beta) = 2\beta(\alpha-1)$ or $H = \frac{N}{4\pi} \frac{A}{\ell\lambda}$ where $A=2b\ (\ell_o-\ell)$. Figure IV-4 shows the function $K(\alpha,\beta)$.

V. SUMMARY

Basic assumptions: (1) Lambertian emitting surface

(2) Single collision with ambient molecules

(3) Isotropic scattering in laboratory frame

Backscattering: $\frac{H}{N} = \frac{2}{5} \frac{(1-\cos^{5/2}\theta)}{\sin^2\theta} \left(\frac{A}{\pi\lambda^2}\right)^{1/2}$, $0 \leq \theta \leq \pi/2$

$\frac{H}{N} = \frac{4}{5} \left(\frac{A}{4\pi\lambda^2}\right)^{1/2}$, $\theta = \pi/2$ (hemispheric beam)

$\frac{H}{N} = \left(\frac{A}{4\pi\lambda^2}\right)^{1/2}$, $\theta = 0$ (cylindrical beam)

Constraints: $\left(\frac{A}{\lambda^2}\right) << 1$

Backscattering to a sphere of radius R:

$\frac{H}{N} = \frac{R}{\lambda}$ cylindrical beam

$\frac{H}{N} = \frac{4}{5} \frac{R}{\lambda}$ hemispherical beam

Scattering from adjacent surfaces

Farfield solution: $\frac{H}{N} = \frac{f}{4\pi} \frac{A_e}{\lambda s}$ independent of emitting cone angle

$$f = \frac{\cos\bar{\theta} + \cos\gamma_s}{1 + \cos\theta_s}$$

Constraints: (1) Receiving area "sees" entire emitting cone

(2) $\frac{A_r}{(r_r)^2_{min}} << 1$

$$(3)\ \overline{\theta}_{min} \geq \overline{\theta} \geq \overline{\theta}_{max}$$

Scattering from a plane to a coplanar point:

$$\frac{H}{N} = \frac{1}{4\pi} \frac{\ell}{\lambda} K(\alpha,\beta)$$

VI. EXAMPLE CALCULATION - LES-8/9

During the launch of LES-8/9, the satellite surfaces will be exposed to molecular fluxes from several sources. Potential contamination of the satellites will occur (1) during enclosure in the payload fairing where the main molecular irradiance source will be the inside fairing surface, (2) between payload fairing jettison and satellite deployment during which the main molecular irradiance source will be the launch vehicle (Transtage), and (3) after satellite deployment. This analysis estimates the molecular irradiance between payload fairing jettison and satellite deployment (a period of about 24,240 seconds) with the goal of assuring that the resulting contamination will not degrade the LES-8/9 operational performance.

The assumptions used in the analysis and discussed in detail later are:

(1) To simplify geometry the satellite surfaces are characterized by a "contamination envelope". Contamination of the envelope is greater than the contamination of the satellite surfaces.

(2) All irradiant molecules condense on the contamination envelope, i.e., none bounce off or are re-emitted (cold surface assumption).

(3) Surfaces not facing each other may exchange molecules by scattering from other surfaces or ambient molecules.

(4) The scattering from ambient molecules is given by the model in the preceeding sections.

(5) The epoxy paint on the surface of the Transtage tanks is the major source of contaminating molecules.

(6) The rate of mass fraction loss of volatile condensible materials (VCM) is 0.1% per 24 hours and assumed to be constant with time.

(7) Contamination is measured by the cumulated surface density deposited on the contamination envelope (gm cm^{-2}).

The profile of the launch vehicle (Transtage) has been shown in Fig. VI-1.[6] The painted surface covering the tanks has been indicated. For a paint thickness of five mils with a density of 1.2 gm cm^{-3}, the amount of paint which can potentially contaminate is about six pounds; however, only a small fraction of this will actually be scattered to the satellite surfaces. Figure VI-2 shows details of the payload stack. For this launch the payload consists of the LES-8/9 satellites and two SOLRAD satellites. Only contamination of LES-8/9 has been considered. In order to simplify the geometry and over-bound the irradiance, LES-8/9 has been replaced by a "contamination envelope" with the shape of a cylinder as shown in Fig. VI-2. Since it is closer to the Transtage the irradiance on this envelope by molecules originating from the sides and bottom of the Transtage over-bounds the irradiance on any of the LES-8/9 surfaces from the same sources.

Figure VI-3 shows some details of the transfer trajectory.[7,8] The Transtage and payload are injected (482 seconds) into an elliptic park orbit of about 80 x 95 nmi . at the end of the State II depletion burn. The Transtage is ignited near parking orbit apogee (4439 seconds) and produces a Hohmann transfer orbit having a synchronous apogee. The Transtage is ignited for the second time (23,705 seconds) to obtain a final circular synchronous orbit with an inclination of 22.84 degrees. The LES-8/9 satellites are deployed (24,555 seconds) followed by the SOLRAD satellites (25,330 seconds).

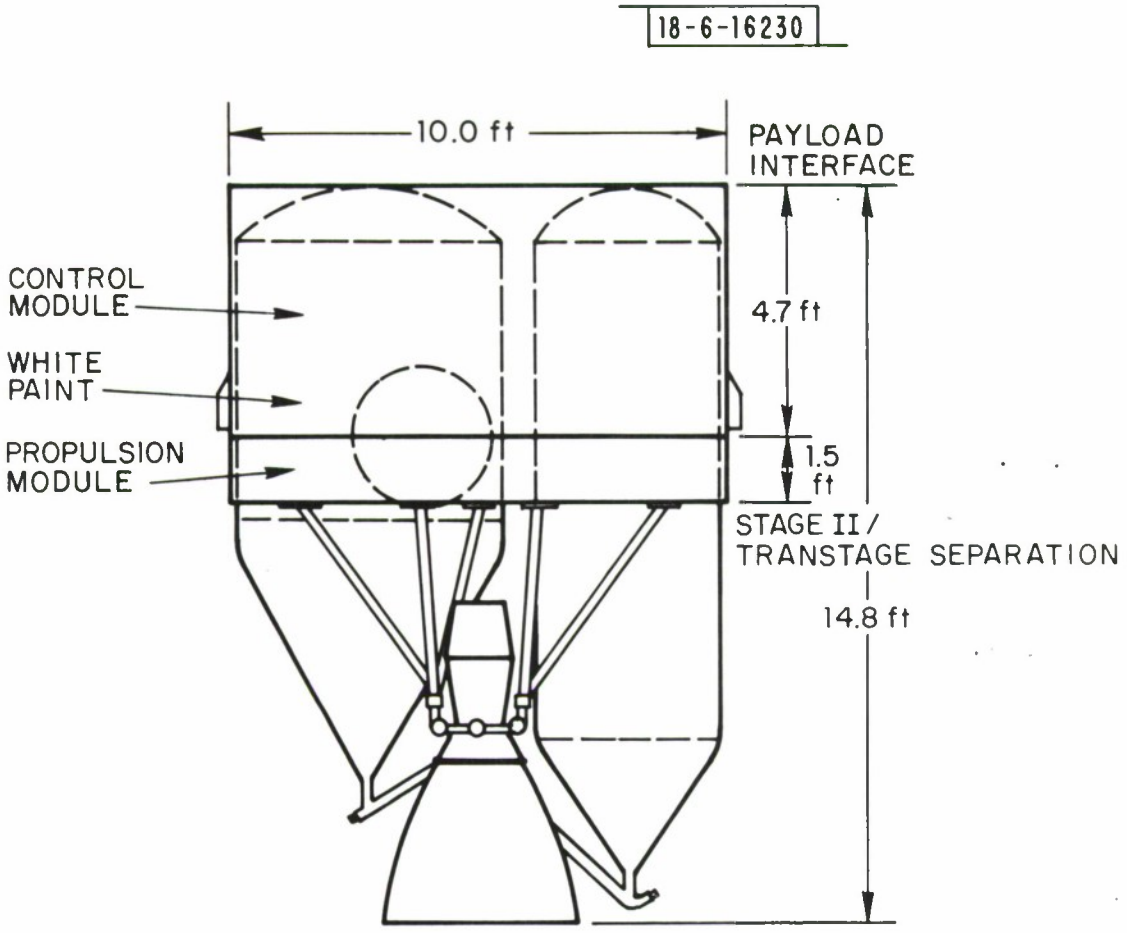

Fig. VI-1. Transtage profile.

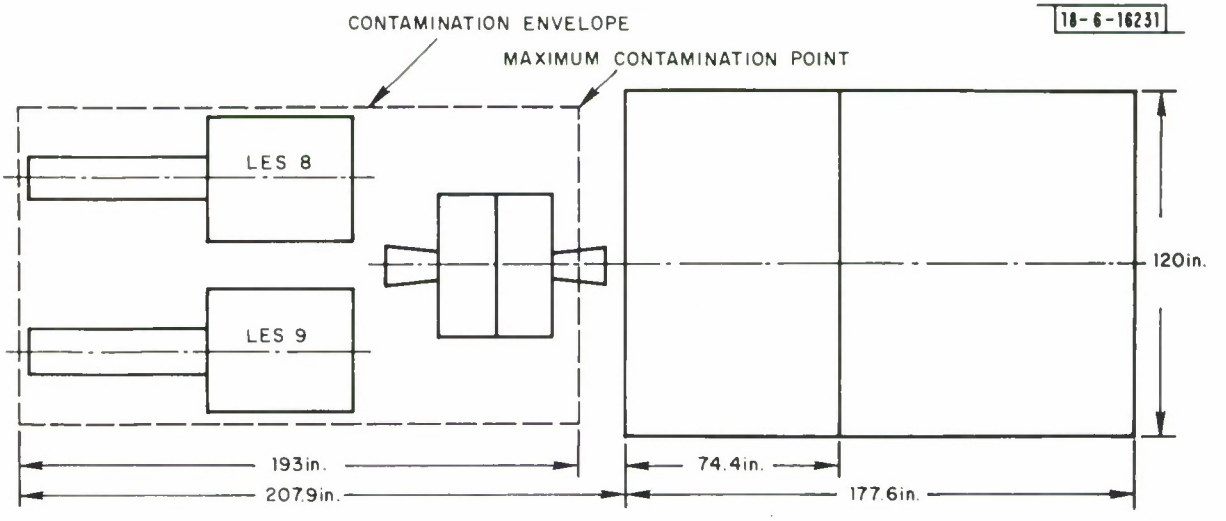

Fig. VI-2. Payload stack details.

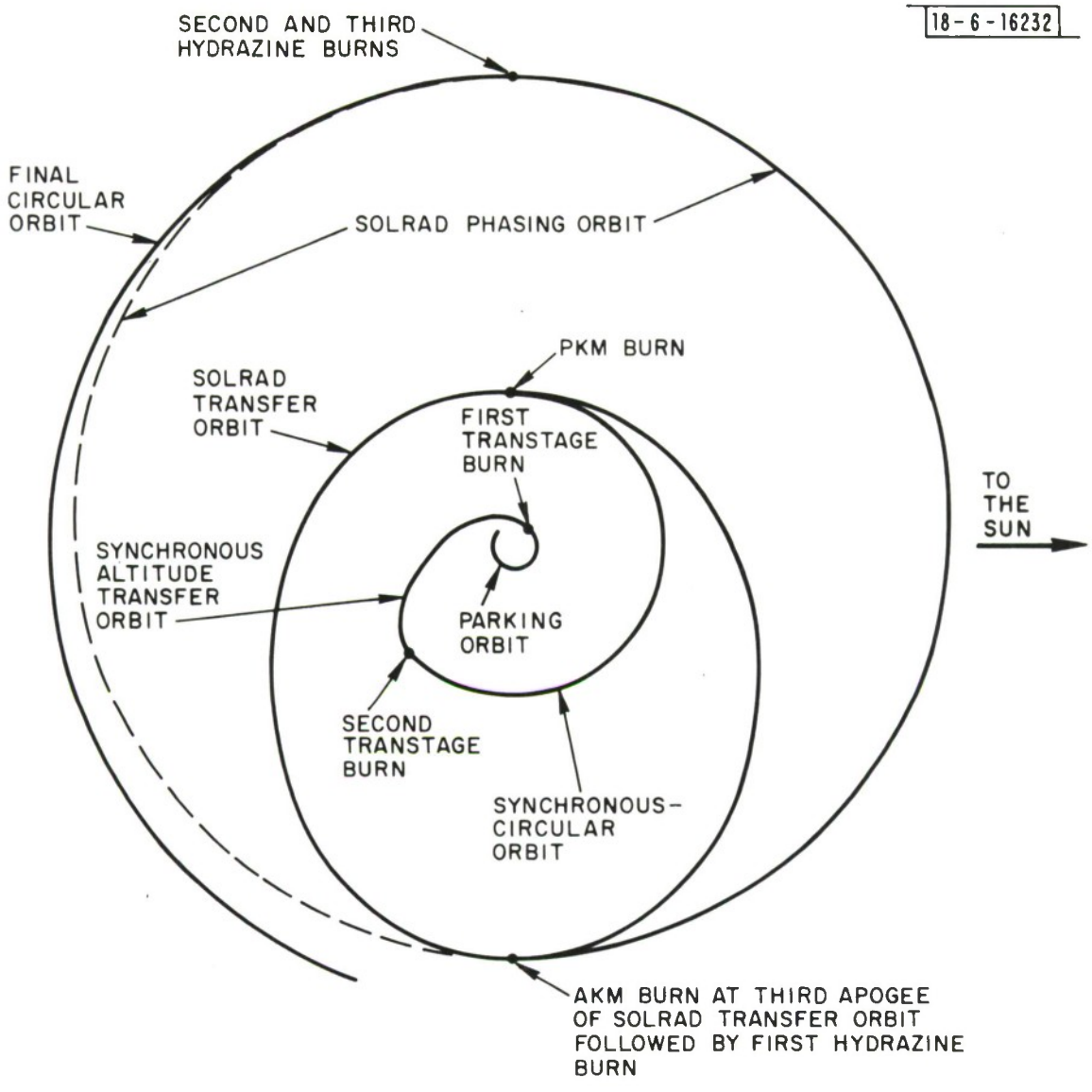

Fig. VI-3. LES-8/9 transfer trajectory.

Based on discussions of the possible contaminating effluxes from the upper stack, it has been assumed that the painted surface of the Transtage is likely to be the largest source of VCM.* Since this surface is close to the LES-8/9 surfaces and is heated during launch, it is likely to be a "dirty" surface which will contaminate to a certain extent the "clean" spacecraft surfaces. From Fig. VI-2 it is seen that the dominant path of molecules originating from surface does not "see" the painted Transtage side. Since the Transtage is downstream of the contamination envelope, the theory in the preceeding sections will over-bound the LES-8/9 contamination.

For the altitudes of interest, scattering of the Transtage molecules to the contamination envelope is in a free-molecular regime, i.e., there is little interaction between the desorbed Transtage molecules and ambient molecules. The ratio of mean free path to a characteristic dimension (Knudsen number) is large. For example, at payload fairing jettison λ = 13 meters and for ℓ = 1 meter, K_n = 13. At higher altitudes the Knudsen number is further increased.

The relative motion between the launch vehicle and ambient molecules is accounted for by the relative mean free path. The relative mean free path is a function of the angle between the launch vehicle velocity and the emitted molecule direction.[1] When this angle is near 90 degrees, which is true for most of the molecules emitted by the Transtage tank surface in parking orbit, $\lambda_{rel} \approx \lambda_{amb}$. Hence, all calculations have assumed ambient mean free paths. If the molecules were emitted into the ambient free stream then $\lambda_{rel} < \lambda_{amb}$.

* Jack Lynch and Ed Murphy, private communications, April 1974.

Assuming a Transtage surface temperature of 100°C, the rate of VCM mass fraction loss (Y) is,[9]

$$Y = 0.1\%/24 \text{ hours} = 1.1574 \times 10^{-8} \text{ sec}^{-1}. \quad (51)$$

The molecular efflux (N) of VCM from the Transtage surface is

$$N = \frac{N_o \delta \rho Y}{W} \quad (\text{molecules cm}^{-2} \text{ sec}^{-1}), \quad (52)$$

where

N_o = Avogadro's number,

δ = paint thickness

ρ = paint density

W = VCM molecular weight.

The contamination is measured by the rate of mass deposited on the contamination envelope. Assuming all the molecules condense or are absorbed on the envelope surface, the contamination rate ($\dot{C}$) is

$$\dot{C} = \frac{HW}{N_o} \quad (\text{gm cm}^{-2} \text{ sec}^{-1}). \quad (53)$$

For simplicity the curved Transtage tank has been replaced with a flat rectangle which is coplanar to the irradiance point. The area of this rectangle has been taken to be one quarter of the total Transtage tank area. This assumption over-bounds the number of molecules scattered to a particular envelope point since the Transtage curvature would reduce the irradiance below the calculated flux. Since the effect of distance on the irradiance goes as 1/s, Transtage surfaces closest to the contamination envelope dominate the irradiance.

Using Eqs. (48) and (52) in Eq. (53) gives,

$$\dot{C} = \frac{\delta \rho Y}{4\pi} \left(\frac{\ell}{\lambda}\right) K(\alpha,\beta) \qquad (54)$$

Note that $\dot{C}$ is independent of the molecular weight of the VCM. The cumulated contamination is the time integral of Eq. (54),

$$C(t) = \int_0^t \dot{C}\, dt. \qquad (55)$$

In Eq. (54) all the parameters have been assumed independent of time except λ which varies according to the trajectory. Figure IV-4 shows the variation of λ with time for the LES-8/9 launch. The maximum envelope contamination takes place closest to the Transtage (Fig. VI-2) and when λ is minimum, i.e., at payload fairing jettison. Table 1 lists the parameters used to compute $\dot{C}$ and C.

TABLE 1

PARAMETERS FOR LES-8/9 CONTAMINATION COMPUTATIONS

Transtage Surface Paint:

δ = 5 mils

ρ = 1.2 gm cm^{-3}

Y = 0.1% per 24 hours

Geometry of Transtage/Envelope:

ℓ = 15 inches	α = 5.96
ℓ_1 = 89.7	β = 2.0
b = 30.0	$K(\alpha,\beta)$ = 6.365

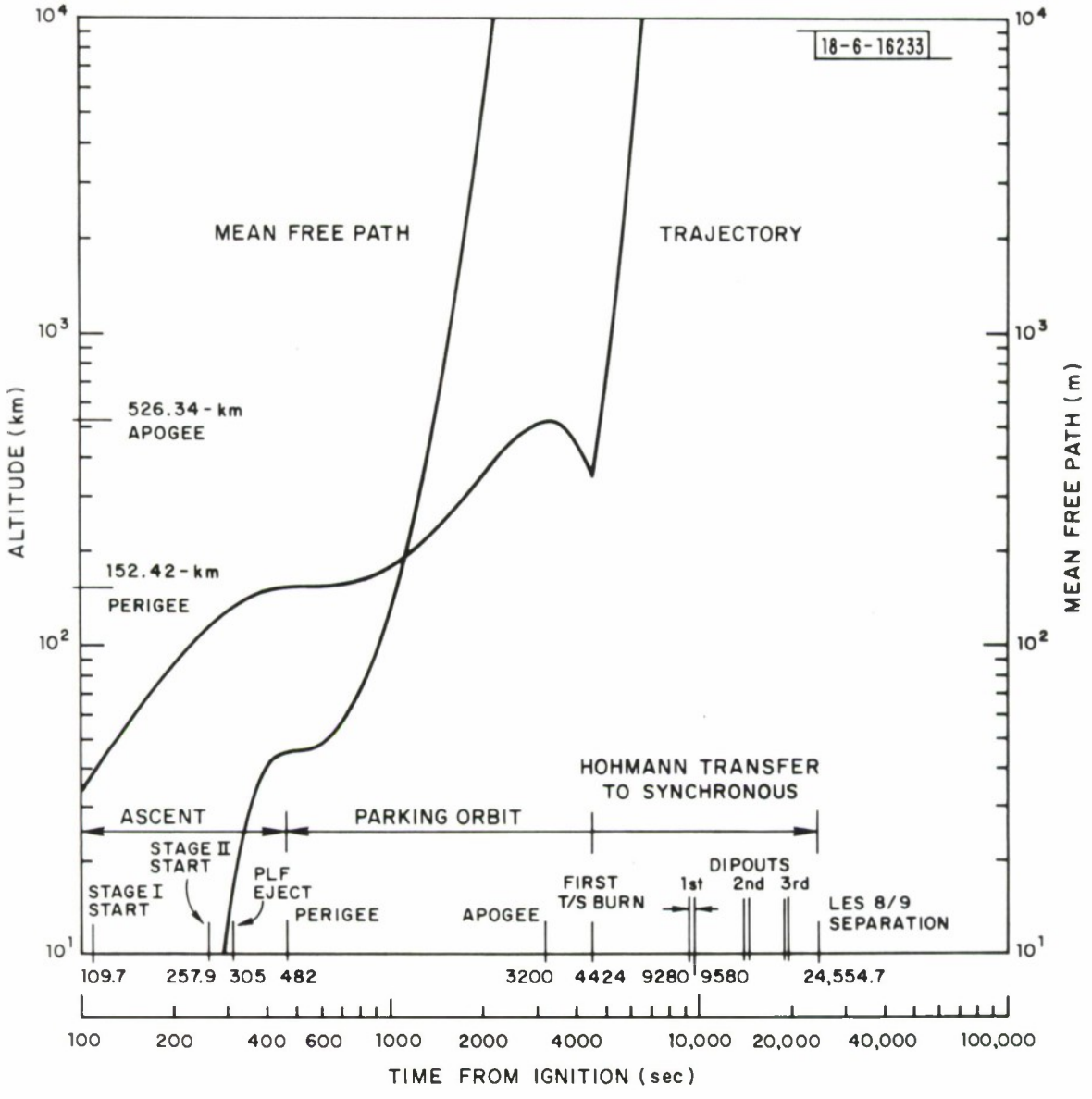

Fig. VI-4. LES-8/9 altitude and mean free path histories.

With the above values, the maximum contamination rate immediately after payload fairing jettision is

$$\dot{C} = \frac{5\times10^{-3} \times 2.54 \times 1.2 \times 1.1574\times10^{-8}}{4\pi} \times 2.94\times10^{-2} \times 6.365$$

$$\dot{C} = 2.638\times10^{-12} \text{ gms cm}^{-2} \text{ sec}^{-1} . \qquad (56)$$

Figure IV-5 shows a plot of the contamination rate and the cumulated contamination as a function of time. Because of the sharp increase in λ with time (Fig. IV-4), the cumulated contamination remains constant after about 1400 seconds from ignition.

The conclusions reached by this analysis are:

(1) The maximum contamination rate from Transtage surface occurs immediately after payload fairing jettison (305 seconds, 133 km altitude).

(2) An upper bound on the maximum cumulated contamination is 5.53×10^{-10} gms cm^{-2} and is reached at about 1400 seconds after ignition.

(3) The contamination collected between payload fairing jettison and satellite deployment is not expected to affect the operational satellite performance.*

---

* A molecular monolayer is about 10^{-8} gm cm^{-2} (H_2O - 1.587×10^{-8} gm cm^{-2}).

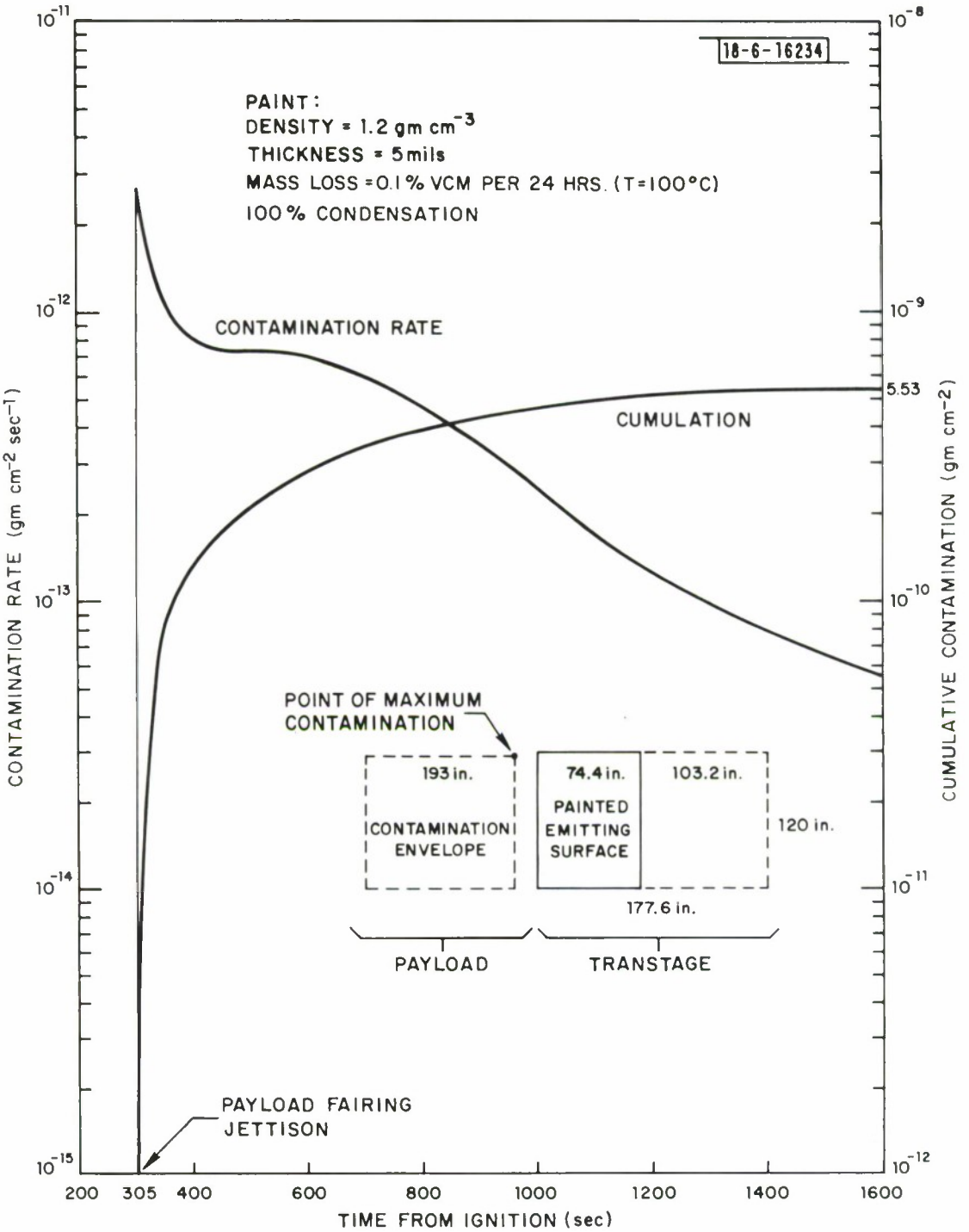

Fig. VI-5. LES-8/9 contamination history.

APPENDIX A

BINARY MOLECULAR COLLISIONS

Basic Equations: Consider a molecule (mass m_i) desorbed from a surface at time t=0 and which travels in a straight line with respect to the surface*. At $t=t_c$ there is a collision with an ambient molecule (mass m_j) resulting, in general, in a new velocity (v_i') and a change in direction (χ'). Figure A-1 shows this scattering process in a frame of reference attached to the emitting surface; this reference frame is referred to as the laboratory frame throughout this report.

The dynamics of colliding molecules are described in part by Newton's laws of motion applied to collections of particles.[10] Summarizing these laws the velocity of the center of mass (v_{cm}) is as if the total system mass (M) were concentrated at the center of mass (CM) and acted upon by the sum of the forces (F) external to the system.

$$\vec{F} = M\vec{v}_{cm}$$

where

$$\vec{F} = \sum_{k=i,j} \vec{F}_k,$$

$$M = \sum_{k=i,j} M_k,$$

$$\vec{v}_{cm} = \sum_{k=i,j} \frac{M_k \vec{v}_k}{M} \quad . \qquad \text{(A-1)}$$

For a system of two colliding particles (m_i,m_j) the collision forces are internal to the system (F = 0), hence

---

* The molecule has the surface velocity plus a velocity with respect to the surface (v_i) which for this analysis has been assumed to be distributed isotropically, i.e., the surface is Lambertian.

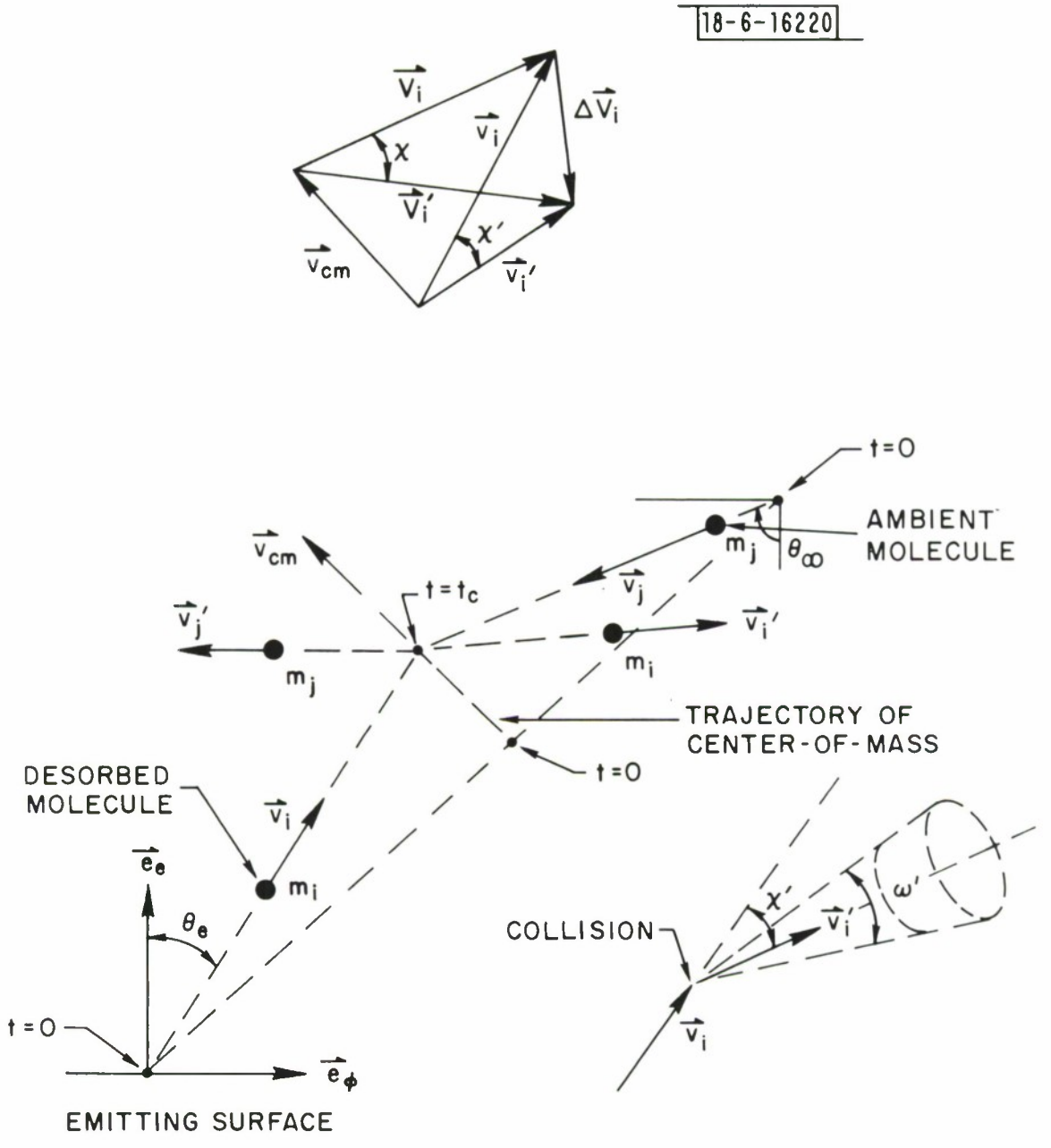

Fig. A-1. Geometry of desorbed/ambient molecular collisions.

$$\vec{v}_{cm} = \sum_{k=i,j} \frac{M_k \vec{v}_k}{M} = \sum_{k=i,j} \frac{M_k \vec{v}_k}{M} = \text{constant.} \qquad \text{(A-2)}$$

The velocity of the molecules relative to the CM is,

$$\vec{V}_k = \vec{v}_k - \vec{v}_{cm} ,$$

$$\vec{V}_k' = \vec{v}_k' - \vec{v}_{cm} , \quad k=i,j \quad . \qquad \text{(A-3)}$$

By definition of the CM, the total system momentum relative to the CM is zero even when $\vec{F} \neq 0$.

$$\sum_{k=i,j} m_k \vec{V}_k = \sum_{k=i,j} m_k \vec{V}_k' = 0 \qquad \text{(A-4)}$$

The total kinetic energy (T) of a system can be written as the kinetic energy due to the total mass moving at $\vec{v}_{cm}$ plus the kinetic energy due to motion relative to the CM.

$$T = \frac{1}{2} M v_{cm}^2 + \sum_{k=i,j} \frac{1}{2} m_k V_k^2 \qquad \text{(A-5)}$$

When $\vec{F} = 0$ and $\vec{v}_{cm}$ = constant, T will be decreased during the collision by internal forces moving through displacements relative to the CM. The total kinetic energy after collision (T′) differs from the intial kinetic energy by the energy which has been absorbed by the internal degrees of freedom of the molecules.

$$T' = \frac{1}{2} M v_{cm}^2 + \sum_{k=i,j} \frac{1}{2} m_k V_k'^2 = T - \Delta E \qquad \text{(A-6)}$$

When $\Delta E=0$, the collision is termed <u>adiabatic</u> and corresponds to no changes in the electronic, vibrational and rotational states of the molecules.

The total angular momentum of a system of particles relative to the CM ($\vec{H}_{cm}$) is related to the moment of the <u>external</u> forces about the center of mass ($\vec{M}_{cm}$).

$$\vec{M}_{CM} = \dot{\vec{H}}_{CM} \quad ,$$

where

$$\vec{M}_{CM} = \sum_{K=i.j} \vec{R}_k \times \vec{F}_k \quad ,$$

$$\vec{H}_{CM} = \sum_{k=i,j} \vec{R}_k \times M_k \vec{V}_k \quad ,$$

$$\vec{R}_k = \vec{r}_k - \vec{r}_{CM} \quad ,$$

$$\vec{r}_{CM} = \sum_{k=i,j} \frac{m_k \vec{r}_k}{M} \quad . \qquad \text{(A-7)}$$

For $\vec{F}_k = 0$,

$$\sum_{k=i,j} \vec{R}_k \times m_k \vec{V}_k = \sum_{k=i,j} \vec{R}_k \times m_k \vec{V}_k' = 0 \quad . \qquad \text{(A-8)}$$

Equations (A-2), (A-4), (A-6) and (A-8) are not sufficient to uniquely determine the resulting velocity ($\vec{V}_k'$) and scattering angle (χ') of the collision. A model for the interaction during collision must be added.

Scattering in the Center-of-Mass System: Figure (A-2) shows the collision geometry in the CM system. Equations (A-4) give

$$m_i V_{it} + m_j V_{jt} = m_i V_{it}' + m_j V_{jt}' = 0 \quad ,$$

$$m_i V_{in} + m_j V_{jn} = M_i V_{in}' + m_j V_{jn}' = 0 \quad . \qquad \text{(A-9)}$$

When the interaction potential has sperical symmetry, the molecules will remain in the plane defined by their initial velocities, i.e., v_i and v_j.

The smooth sphere model gives,

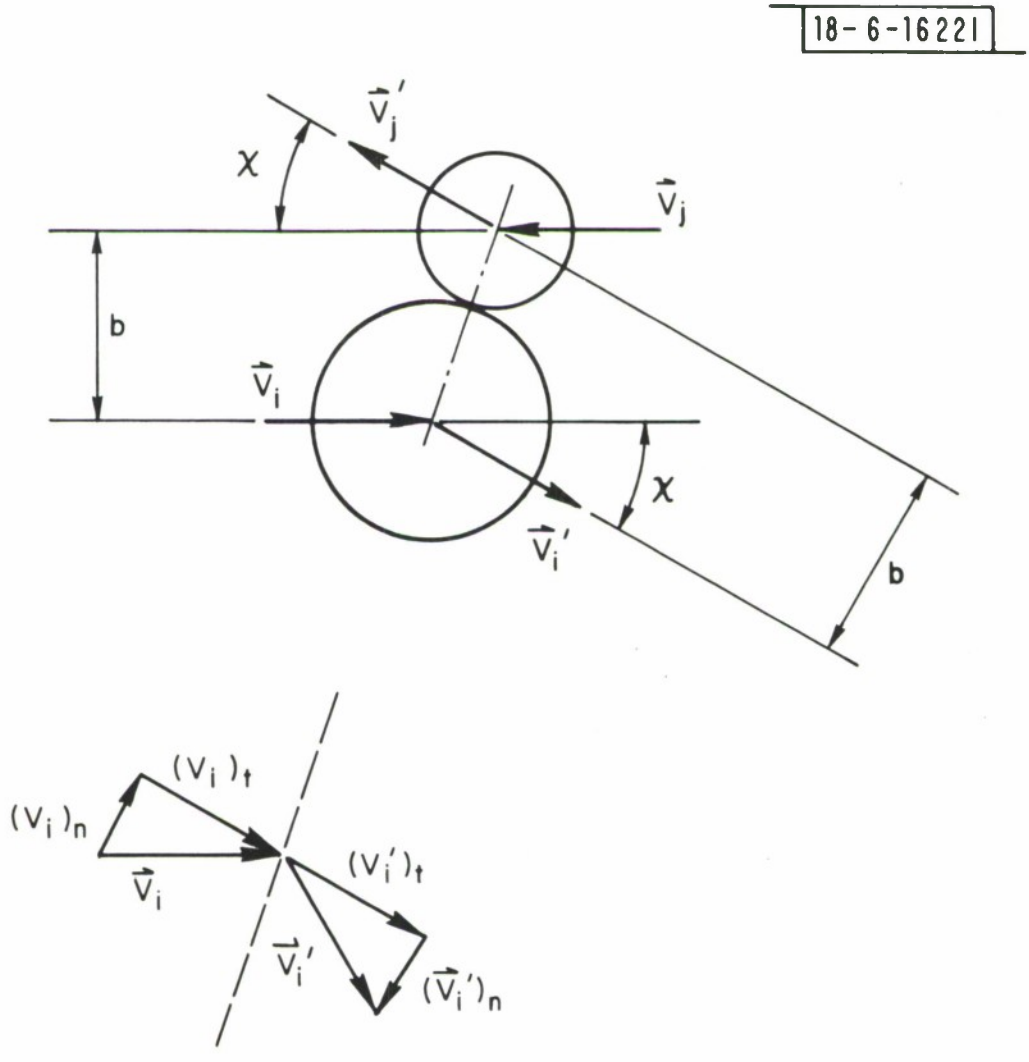

Fig. A-2. Collisions of hard spheres in the center of mass system.

$$V'_{kt} = V_{kt} \quad , \; k=i,j \quad . \tag{A-10}$$

To solve for V'_{in} and V'_{jn} let

$$V'_{jn} - V'_{in} = e(V_{in}-V_{jn})$$

where $0 \leq e \leq 1$.

The coefficient of restitution (e) measures the degree that the collision departs from an adiabatic one. For e=0, the collision is inelastic (non-adiabatic) and for e=1, the collision is perfectly elastic (adiabatic).

Solving Eqs. (A-9) and (A-11) gives,

$$V'_{kn} = -eV_{kn} \quad , \; k=i,j \quad . \tag{A-12}$$

The scattering angle of the i^{th} molecule in the CM system is found from,

$$\cos \chi = \frac{\vec{V}_i \cdot \vec{V}_i}{V_i \cdot V_i} \quad ,$$

where

$$\vec{V}_i = V_{it}\vec{e}_t + V_{in}\vec{e}_{in} \; ,$$
$$\vec{V}'_i = V'_{it}\vec{e}_t + V'_{in}\vec{e}_n \quad . \tag{A-13}$$

For the smooth sphere model,

$$\cos \chi = \frac{\left(\frac{V_{it}}{V_i}\right)^2 - e\left(\frac{V_{in}}{V_i}\right)^2}{\left(\frac{V'_i}{V_i}\right)} \quad , \tag{A-14}$$

In terms of the collision parameter (b) and collision cross-section (σ) (Fig. A-2),

$$\cos \chi = \frac{\sin^2\sigma - e \cos^2\theta}{(\sin^2\theta + e^2 \cos^2\theta)^{1/2}} ,$$

where

$$\sin \theta = \bar{b} \quad , \qquad \bar{b} = b/\sigma \tag{A-15}$$

Hence,

$$\cos \chi = \frac{(1+e)\bar{b}^2 - e}{[(1-e^2)\bar{b}^2 + e^2]^{1/2}} \quad , \tag{A-16}$$

and

$$\left(\frac{V_i'}{V_i}\right)^2 = (1-e^2)\bar{b}^2 + e^2 \quad . \tag{A-17}$$

For e=1 (adiabatic)

$$\cos \chi = 2\bar{b}^2 - 1, \quad , \bar{b} \leq 1,$$
$$= 1 \qquad , \bar{b} > 1,$$

$$V_i' = V_i \ . \tag{A-18}$$

For e=0 (inelastic)

$$\cos \chi = \bar{b} \quad , \bar{b} \leq 1 \quad ,$$
$$= 1 \quad , \bar{b} > 1$$

$$V_i' = \bar{b} V_i \ . \tag{A-19}$$

Generalizing the smooth sphere model, for adiabatic collisions with spherically symmetrical interaction potentials, Hirschfelder, et al.[11] gives for the CM scattering angle,

$$\chi(b,g) = \pi - 2b \int_{r_m}^{\infty} \frac{\frac{dr}{r^2}}{\left(1 - \frac{\phi}{\frac{1}{2}\mu g^2} - \frac{b^2}{r^2}\right)^{1/2}} \quad , \qquad \text{(A-20)}$$

where

r_m = minimum distance between the molecules during the collision

$\phi(r)$ = interaction potential

g = initial relative speed.

The elastic sphere (e=1) is then given by,

$$\begin{aligned} \phi(r) &= \infty \quad , \quad r < \sigma \quad , \\ &= 0 \quad , \quad r > 0 \quad , \\ r_m &= \sigma \quad , \quad b \leq \sigma \quad , \\ &= b \quad , \quad b \geq \sigma \quad . \end{aligned} \qquad \text{(A-21)}$$

and yields Eqs. (A-18) upon integration.

In summary, for adiabatic collisions there is no energy loss (by definition), the speeds in the CM system are unchanged, the collision is completely described by Eq. (A-20) for spherical potentials, χ is the same for both particles and the impact parameters are unchanged. Non-adiabatic collisions have been modeled by smooth spheres with the coefficient of restitution.

LES-8/9 Scattering in the Laboratory System: The speed of the ambient molecules was taken to be equal to the speed of the launch vehicle. The speed of the desorbed molecules with respect to the emitting surface was taken as the mean thermal speed evaluated at the surface temperature (100°C). Table 2

shows the desorbed/ambient momentum ratios for the LES-8/9 launch at an altitude of 132.55 km (305 seconds after ignition) for a range of desorbed molecular weights. While the desorbed molecules are more massive they travel sufficiently slow so that the ambient molecules have more momentum.

TABLE 2

MOMENTUM OF DESORBED AND AMBIENT MOLECULES

(LES-8/9 launch - 132.55 km)

Desorbed Molecular Weight	Desorbed Thermal Velocity*	Desorbed/Ambient Momentum Ratio**
1000	8.8866×10^{-2} km/sec	0.6149
500	1.255×10^{-1}	0.4348
100	2.8101×10^{-1}	0.1944
50	3.9742×10^{-1}	0.1375

* $T = 100°C$

** $W_{amb} = 27.5$, $V_{amb} = 5.255$ km/sec

Figure II-3 schematically shows the scattering of a desorbed molecule emitted at 45° to the surface normal by an ambient molecule traveling parallel to the surface. The figure corresponds to a typical collision during the LES-8/9 launch when both molecules are modeled by perfectly elastic, smooth spheres. As shown in the preceding subsections for this model, the desorbed molecules are scattered uniformly over a sphere centered at $\vec{v}_1 + \vec{v}_{CM}$, i.e.,

isotropically with respect to the center of mass system. Figure II-3 shows that the assumption of isotropic scattering in the laboratory system will underestimate the number of molecules scattered in the forward and downstream directions while over-estimating the number scattered in the backward and upstream directions. The equations developed in Sections II through IV therefore overbound the molecular irradiance on upstream surfaces of the spacecraft.

APPENDIX B

EVALUATION OF SOME INTEGRALS

In Section III-A (p. 13) it was shown that the molecular irradiance due to backscattering from a cylindrical beam was a function of the following integral,

$$I_1(\varepsilon) = \int_0^\infty dx \, \exp(-x) \left[1 - \frac{x}{(x^2+\varepsilon^2)^{1/2}}\right] . \tag{B-1}$$

It is desired to evaluate Eq. (B-1) for $\varepsilon << 1$. From Gradshteyn and Ryshik[5] Eq. (B-1) is

$$I_1(\varepsilon) = 1 - \left\{\frac{\pi}{2}\,\varepsilon\left[H_1(\varepsilon) - N_1(\varepsilon) - \varepsilon\right]\right\} . \tag{B-2}$$

where H_1 = Struve function first order

N_1 = Neumann function first order .

By definition

$$H_1(\varepsilon) = \sum_{m=o}^{\infty} \frac{(-)^m (\frac{\varepsilon}{2})^{2+2m}}{\Gamma(m+3/2)\ \Gamma(m+5/2)}$$

$$\pi N_1(\varepsilon) = 2J_1(\varepsilon)\ (\ell n\ \frac{\varepsilon}{2} + C) - \frac{2}{\varepsilon} - \frac{\varepsilon}{2}$$

$$- \sum_{k=1}^{\infty} \frac{(-)^k (\frac{\varepsilon}{2})^{1+2k}}{k!\ (k+1)!} \left[\sum_{m=1}^{1+k} \frac{1}{m} + \sum_{m=1}^{k} \frac{1}{m}\right] \tag{B-3}$$

where C = Euler's constant and J_1 is the Bessel function of the first kind. Writing out the first few terms of (B-3) and substituting in (B-2) gives

$$I_1(\varepsilon) = 1 + \varepsilon - \frac{\pi}{2}\,\varepsilon\left[\frac{(\frac{\varepsilon}{2})^2}{\Gamma(\frac{3}{2})\ \Gamma(\frac{5}{2})} - \frac{(\frac{\varepsilon}{2})^4}{\Gamma(\frac{5}{2})\ \Gamma(\frac{7}{2})} + \ldots\right.$$

$$- \frac{2}{\pi}\, J_1(\varepsilon)\ (\ell n\ \frac{\varepsilon}{2} + C) + \frac{1}{\pi}\ (\frac{2}{\varepsilon}) + \frac{1}{\pi}\ (\frac{\varepsilon}{2})$$

$$\left. - \frac{1}{2!}\ (\frac{\varepsilon}{2})^3\ (\frac{3}{2}) + \ldots\right] \qquad \text{(B-4)}$$

For $\varepsilon << 1$

$$I_1(\varepsilon) = 1 + \varepsilon - \frac{\pi}{2}\ \varepsilon\ (\frac{1}{\pi}\,\frac{2}{\varepsilon}) + O(\varepsilon^2) \qquad \text{(B-5)}$$

or

$$I_1(\varepsilon) \approx \varepsilon \quad . \qquad \text{(B-6)}$$

For ε small $I_1(\varepsilon)$ is determined mainly by values of the integrand near $x = 0$. Hence, bounding exp (-x) by unity and integrating gives the first term in the expansion of the exact solution.

In Section IV-A (p. 20) it was shown that the far-field solution for the molecular irradiance was a function of the following integral,

$$I_\omega = \int\int_{\substack{\text{emitting}\\ \text{cone}}} d\omega\, \cos\theta_e\, \frac{(\vec{e}_s \cdot \vec{e}_r + \vec{e}_\omega \cdot \vec{e}_r)}{(1 + \vec{e}_\omega \cdot \vec{e}_s)} \quad . \qquad \text{(B-7)}$$

Using the coordinate system shown in Fig. IV-1 it can be shown that

$$\vec{e}_s \cdot \vec{e}_r = \cos\gamma_s$$

$$1 + \vec{e}_\omega \cdot \vec{e}_s = a + b\,\cos\phi_e$$

$$\vec{e}_\omega \cdot \vec{e}_r = c + d\,\cos\phi_e + e\,\sin\phi_e \qquad \text{(B-8)}$$

where

$$a = 1 + \cos\theta_s \cos\theta_e$$

$$b = -\sin\theta_s \sin\theta_e$$

$$c = \cos\bar{\theta} \cos\theta_e$$

$$d = \sin\bar{\theta} \cos\bar{\phi} \sin\theta_e$$

$$e = \sin\bar{\theta} \sin\bar{\phi} \sin\theta_e$$

Eq. (B-7) becomes

$$I_\omega = \int_o^\theta d\theta_e \sin\theta_e \cos\theta_e I_\phi(\theta_e) \qquad \text{(B-9)}$$

where

$$I_\phi(\theta_e) = I_1 + I_2 + I_3$$

$$I_1 = (\cos\gamma_s + c) \int_o^{2\pi} \frac{d\phi_e}{a + b\cos\phi_e}$$

$$I_2 = d \int_o^{2\pi} \frac{d\phi_e \cos\phi_e}{a + b\cos\phi_e}$$

$$I_3 = e \int_o^{2\pi} \frac{d\phi_e \sin\phi_e}{a + b\cos\phi_e}$$

Evaluating I_1, I_2, and I_3 gives

$$I_\phi(\theta_e) = \frac{2\pi(\cos\gamma_s + c)}{(a^2 - b^2)^{1/2}} + 2\pi\frac{d}{b} - \frac{2\pi\frac{ad}{b}}{(a^2 - b^2)^{1/2}} \quad . \qquad \text{(B-10)}$$

Substituting (B-10) in (B-9) gives

$$I_\omega = 2\pi \left\{ - \frac{\sin\bar{\theta}\,\cos\bar{\phi}}{\sin\theta_s} \frac{\sin^2\theta}{2} \right.$$

$$+ \left(\cos\gamma_s + \frac{\sin\bar{\theta}\,\cos\bar{\phi}}{\sin\theta_s}\right) \left[1 - \cos\theta - \cos\theta_s \ln\left(\frac{1 + \cos\theta_s}{\cos\theta + \cos\theta_s}\right)\right]$$

$$+ \left(\cos\bar{\theta} + \frac{\sin\bar{\theta}\,\cos\bar{\phi}\,\cos\theta_s}{\sin\theta_s}\right)$$

$$\left. \cdot \left[\frac{\sin^2\theta}{2} - \cos\theta_s\,(1 - \cos\theta) + \cos^2\theta_s \ln\left(\frac{1 + \cos\theta_s}{\cos\theta + \cos\theta_s}\right)\right]\right\} . \quad \text{(B-11)}$$

Letting

$$I_\omega = \frac{N}{I} f \quad , \quad \text{(B-12)}$$

where for a Lambertian surface

$$N = \pi I \sin^2\theta .$$

$$f = \left\{ - \frac{\sin\bar{\theta}\,\cos\bar{\phi}}{\sin\theta_s} \right.$$

$$+ 2\left(\cos\gamma_s + \frac{\sin\theta\,\cos\phi}{\sin\theta_s}\right) \left[\frac{1 - \cos\theta}{\sin^2\theta} + \frac{\cos^2\theta}{\sin^2\theta} \ln\left(\frac{1 + \cos\theta_s}{\cos\theta + \cos\theta_s}\right)\right]$$

$$+ \left(\cos\bar{\theta} + \frac{\sin\bar{\theta}\,\cos\bar{\phi}\,\cos\theta_s}{\sin\theta_s}\right) \left[1 - \frac{2(1 - \cos\theta)}{\sin^2\theta} \cos\theta_s \right.$$

$$\left. \left. + \frac{2\cos^2\theta_s}{\sin^2\theta} \ln\left(\frac{1 + \cos\theta_s}{\cos\theta + \cos\theta_s}\right)\right]\right\} \quad . \quad \text{(B-13)}$$

Multiplying out and collecting terms simplifies (B-13) to

$$f = \frac{\cos\bar{\theta} + \cos\gamma_s}{1 + \cos\theta_s} \quad . \quad \text{(B-14)}$$

NOMENCLATURE

A	Area	cm^2
b	Surface dimension (Fig. IV-4)	cm
	Collision parameter	cm
C	Surface contamination	gm cm^{-2}
$\dot{C}$	Time rate of change of C	gm cm^{-2} sec^{-1}
$\vec{e}$	Area normal unit vectors	
H	Molecular irradiance	molecules cm^{-2} sec^{-1}
I	Molecular specific intensity	molecular cm^{-2} sec^{-1} str^{-1}
$K(\alpha,\beta)$	Geometric factor for scattering from a plane	----
K_n	Knudsen number	----
ℓ, ℓ_o	Lengths (Fig. IV-4)	cm
M,m	Molecular mass	gm
N	Emitted molecular flux	molecules cm^{-2} sec^{-1}
N_o	Avogadro's number	molecules $moles^{-1}$
r	Radial coordinate	cm
s	Distance between emitting and receiving areas	cm
S	Nondimensional s	cm
t	Time	sec
v	Velocity	cm sec^{-1}
V	Volume	cm^3
V_{amb}	Velocity of satellite	km sec^{-1}
W	Molecular weight	gm $mole^{-1}$
$\dot{Y}$	Time rate of changes of paint coating mass fraction	sec^{-1}
x	Nondimensional r_e	----

y	Nondimensional r_r	---
α, β	Nondimensional lengths (Eq. 49)	---
δ	Paint thickness	mils
ε	Eq. (17)	---
γ	Eq. (24)	---
λ	Mean free path	cm
ρ	Paint density	gm cm^{-3}
	Eq. (16)	cm
θ	Polar angle	deg.
ϕ	Azimuth angle	deg.
χ, χ'	Center of mass and laboratory scattering angles	deg.
ω	Emitting solid angle	str
ω'	Receiving area solid angle	str

Subscripts

e	Emitting area
r	Receiving area
rel	Relative
amb	Ambient

ACKNOWLEDGMENT

The author would like to acknowledge the assistance given by his M.I.T. Lincoln Laboratory colleagues Dr. Jack T. Lynch who originally suggested the problem and provided many useful suggestions and Mr. Chris H. Moulton who did the computer work.

REFERENCES

1. J. J. Scialdone, "Self Contamination and Environment of an Orbiting Spacecraft," NASA TN D-6645 (May 1972).

2. J. S. Scialdone, "Predicting Spacecraft Self-Contamination in Space and in a Test Chamber," NASA TN D-6682 (May 1972).

3. A. L. Lee and S. J. Robertson, "Mathematical Model of Molecular Flow in the NASA-JSC Thermal-Vacuum Chamber A," Paper No. 63, Seventh Conference on Space Simulation, NASA SP-336 (November 1975).

4. W. L. Wolfe, ed., "Handbook of Military Infrared Technology," Superintendent of Documents (U. S. Government Printing Office 1965), Ch. 1.

5. I. S. Gradshteyn and I. M. Ryshik, Table of Integrals, Series and Products (Academic Press, New York, 1965).

6. "Titan III Performance and Characteristic Handbook (Rev. 1)," Martin Marietta Corporation, M-70-7 (January 1973).

7. R. Bobrow, "P74-1 Mission Requirements and Constraints," TRW memorandum No. D00601-1 (October 1973), p. 4.

8. "P74-1 Mission Planning Trajectory (Rev. 1)," Martin Marietta Corporation, MCR-73-204 (September 1973).

9. R. F. Muraca, et al., "Polymers for Spacecraft," MTIS, U96625A (September 1967).

10. D. T. Greenwood, Principles of Dynamics (Prentice-Hall, New York, 1965), Ch. 4.

11. J. O. Hirschfelder, C. F. Curtiss and R. B. Bird, Molecular Theory of Gases and Liquids (Wiley, New York, 1954), p. 51.

REPORT DOCUMENTATION PAGE		READ INSTRUCTIONS BEFORE COMPLETING FORM
1. REPORT NUMBER ESD-TR-75-147	2. GOVT ACCESSION NO.	3. RECIPIENT'S CATALOG NUMBER
4. TITLE *(and Subtitle)* Spacecraft Self-Contamination by Molecular Outgassing		5. TYPE OF REPORT & PERIOD COVERED Technical Note 6. PERFORMING ORG. REPORT NUMBER Technical Note 1975-1
7. AUTHOR*(s)* Harvey, Robert L.		8. CONTRACT OR GRANT NUMBER*(s)* F19628-73-C-0002
9. PERFORMING ORGANIZATION NAME AND ADDRESS Lincoln Laboratory, M.I.T. P.O. Box 73 Lexington, MA 02173		10. PROGRAM ELEMENT, PROJECT, TASK AREA & WORK UNIT NUMBERS Project No. 649L
11. CONTROLLING OFFICE NAME AND ADDRESS Air Force Systems Command, USAF Andrews AFB Washington, DC 20331		12. REPORT DATE 31 March 1975 13. NUMBER OF PAGES 66
14. MONITORING AGENCY NAME & ADDRESS *(if different from Controlling Office)* Electronic Systems Division Hanscom AFB Bedford, MA 01731		15. SECURITY CLASS. *(of this report)* Unclassified 15a. DECLASSIFICATION DOWNGRADING SCHEDULE

16. DISTRIBUTION STATEMENT *(of this Report)*

Approved for public release; distribution unlimited.

17. DISTRIBUTION STATEMENT *(of the abstract entered in Block 20, if different from Report)*

18. SUPPLEMENTARY NOTES

None

19. KEY WORDS *(Continue on reverse side if necessary and identify by block number)*

satellite communications
survivable satellites
spacecraft contamination
molecular outgassing
LES-8
LES-9

20. ABSTRACT *(Continue on reverse side if necessary and identify by block number)*

The contamination of spacecraft surfaces from ambient and outgassing molecules is considered. A model is formulated for the molecules desorbed from the spacecraft surfaces and scattered by the ambient molecules back to the emitting and adjacent surfaces. Equations are derived for the back-scatter and far-field cases as a function of surface geometry, mean free path, and desorbing beam shape. Expressions are given for point to point and flat surface to point scattering. The scattered molecular irradiance is combined with other sources to obtain the total molecular irradiance. A calculation of the contamination during launch of the Lincoln Experimental Satellites 8 and 9 is given.